Title
Fabrication and Characterization of Nanomagnetic Media for Data Storage and Logic Operations

Author
Butler, John Stephen

Publication Date
2014

UNIVERSITY OF CALIFORNIA
RIVERSIDE

Fabrication and Characterization of Nanomagnetic Media for Data Storage and Logic Operations

A Dissertation submitted in partial satisfaction
of the requirements for the degree of

Doctor of Philosophy

in

Electrical Engineering

by

John Stephen Butler

December 2014

Dissertation Committee:
Dr. Ilya Dumer, Chairperson
Dr. Sakhrat Khizroev
Dr. Nissim Amos

The Dissertation of John Stephen Butler is approved:

____

____

____

Committee Chairperson

University of California, Riverside

ACKNWOLEDGEMENTS

Professors: Sakhrat Khizroev, Nissim Amos, and Ilya Dumer. National Science Foundation (NSF), Department of Defense (DoD), Defense MicroElectronics Activity (DMEA), all my colleagues at the at UCR (listed in the order of their first name): Beomseop Lee, Bing Hu, Chen Zang, Davil Garcia, Frederick Gertz, Jeongmin Hong, Meir Shachar, Rabee Ikkawi, Robert Fernandez, Steven Chen, and Yuan Tian. Special thanks to Dexter Humphrey for all of the help in the Center for Nanoscale Science & Engineering (CNSE) cleanroom.

Portions of the materials presented in this dissertation were reproduced with permission from the following publications:

- B. Hu, N. Amos, Y. Tian, **J. Butler**, D. Litvinov, and S. Khizroev, “Study of Co/Pd multilayers as a candidate material for next generation magnetic media,” *J. Appl. Phys.*, vol. 109, no. 3, p. 034314, Feb. 2011. Copyright 2011, AIP Publishing LLC.

- N. Amos, **J. Butler**, B. Lee, M. H. Shachar, B. Hu, Y. Tian, J. Hong, D. Garcia, R. M. Ikkawi, R. C. Haddon, D. Litvinov, and S. Khizroev, “Multilevel-3D Bit Patterned Magnetic Media with 8 Signal Levels Per Nanocolumn,” *PLoS One*, vol. 7, no. 7, p. e40134, Jan. 2012.

- **J. Butler**, M. Shachar, B. Lee, D. Garcia, B. Hu, J. Hong, N. Amos, and S. Khizroev, “Reconfigurable and non-volatile vertical magnetic logic gates,” *J. Appl. Phys.*, vol. 115, no. 16, p. 163903, Apr. 2014. Copyright 2014, AIP Publishing LLC.

- N. Amos, E. Stefanescu, **J. Butler**, B. Lee, Y. Tian, R. Ikkawi, R. Chomko, V. L. Safonov, R. Haddon, D. Litvinov, and S. Khizroev, “Three-Dimensional Non-Volatile Magnetic Universal Logic Gates,” *J. Nanoelectron. Optoelectron.*, vol. 6, no. 2, pp. 132–137, Jun. 2011.

DEDICATION

I dedicate my work to my family. To my wife Maggie for being patient and supportive of me during my time as a graduate student. And to my parents for everything that they have done to support me during my collegiate career. Thank you all for everything that you have done for me.

ABSTRACT OF THE DISSERTATION

Fabrication and Characterization of Nanomagnetic Media for Data Storage and Logic Operations

by

John Stephen Butler

Doctor of Philosophy, Graduate Program in Electrical Engineering
University of California, Riverside, December 2014
Dr. Ilya Dumer, Chairperson

In recent years, current data storage and semiconductors have begun to reach their fundamental limits. In current hard disk drive based data storage technology the size of the magnetic bit that data is stored on has begun to reach it size limits due to the superparamagnetic limit. In semiconductor technologies, devices are beginning to reach their fundamental limits due to the current leakage effect in small devices. If these technologies will continue with the current trends of packing more data/devices into the same area, new technologies need to be developed. In the following pages, two new technologies will be proposed for increasing the areal density of magnetic data storage technologies. After that, three novel approaches to creating logic cells on patterned magnetic media at much higher areal densities than current semiconductor technologies can support. First a study of Co/Pd multilayers as a candidate material for the next generation of magnetic media for a number of applications will be described. Following that, a patterned, three layer, magnetic media made up of magnetic multilayers will be fabricated and tested to show the feasibility of using it for the basis of next generation data storage technologies. Then, three novel approaches to magnetic logic gates using magnetic multilayers based media will be designed, fabricated, and tested using state of the art fabrication and analysis techniques. Each of the proposed magnetic logic cells will consist of a patterned media made up on of two, three, or four stacked magnetic multilayers media. The two layer structures are fabricated to be implemented on current hard disk drives. The three and four stacked structures can be implemented in a number of ways, from hard disk drives to magnetic quantum-dot cellular automata. The latter would allow these logic cells to be integrated with semiconductor technologies to create a hybrid device that utilizes the best aspects of each technology.

Table of Contents

Section 1 – Data Storage 1
Introduction 1
Study of Co/Pd Multilayers 4
Introduction 4
Experiment 5
Results and Discussion 6
Conclusion 16
Multilevel-3D Bit Patterned Magnetic Media with 8 Signal Levels Per Nanocolumn. 17
Introduction 17
Materials and Methods 20
Results and Discussion 24
Conclusion 33
Section 2 - Logic 35
Introduction 35
Overview of Computer Logic 36
Background 37
Transistors 38
Magnetic Logic 39
Multilevel Patterned Magnetic Media for HDD-based Nanomagnetic Logic 41
Introduction 41
Concept 42
Fabrication 45
Magnetic Force Microscopy (MFM) Study 47
Conclusion 51
Reconfigurable and Non-Volatile Vertical Magnetic Logic Gates 52
Introduction 52
Concept 52
Fabrication 57
Magnetic Force Microscopy (MFM) Study 58
Conclusion 62

Three-dimensional Non-Volatile Magnetic Universal Logic Gates 64
Introduction 64
3-D Logic Devices.. 65
Conclusions 73
Section 3 - Conclusion... 75
Section 4 - References 77

Table of Figures

Figure 1: AFM images (5 X 5 μm^2) of a Si substrate (a) prior to Ar^+ milling, (b) after Ar^+ milling with roughness (Ra) values of 0.791 nm and 0.077 nm, respectively. The roughness measurements were taken from the high-lighted rectangular frames, (c) A comparison of hysteresis loops for Co/Pd MLs deposited on Si substrates with and without Ar^+ milling. 7
Figure 2: Hysteresis loops of Co/Pd MLs on Si substrate with the variance of Co bilayer thickness. 8
Figure 3: Coercivity behavior of Co/Pd MLs on Si substrate as a function of Co-bilayer thickness. 9
Figure 4: Hysteresis loops of Pd(5 nm)/[Co(0.26 nm)/Pd(y nm)]$_7$/Pd(5 nm) on Si substrate with the variance of Pd bilayer thickness. 9
Figure 5: Hysteresis loops of Co/Pd MLs deposited at different processing pressures. .. 10
Figure 6: MFM images (5 X 5 μm^2) of demagnetized samples with different processing pressure on Si substrate (a) 5 mTorr, (b) 15 mTorr. 12
Figure 7: Coercivity behavior of Co/Pd MLs as a function of the number of Co/Pd MLs (n). 13
Figure 8: Major and minor hysteresis loops of three stack Co/Pd MLs on silicon substrate. 15
Figure 9: MFM images (5 X 5 μm^2) of single-stack Co/Pd MLs media for two, seven, and ten bilayers and a triple-stack Co/Pd MLs media exhibiting all three layers together, starting with the ten bilayers stack in the bottom and the two bilayers stack at the top. .. 15
Figure 10: Triple-stack ML-3D BPM. Schematic of the structure and desired magnetic properties (not to scale). The black arrows (binary "1″) and red arrows (binary "0″) denote the two possible magnetic states in each stack. Above the columns lies the binary representation and color coding for the eight possible magnetic states. 20
Figure 11: ML-3D magnetic media composition. 21
Figure 12: ML-3D BPM media fabrication process. (a) Sputter-deposition of the triple-stack ML-3D magnetic media composition, (b) Spin-coat and bake HSQ, (c) E-beam lithography (expose and develop patterns), (d) ICP etching of the naturally oxidized Ti layer, (e) Ar-ion milling of the remaining composition to form the triple-stack ML-3D BPM. 23
Figure 13: MOKE hysteresis loop. A graph revealing three magnetically-decoupled recording layers for the fabricated ML-3D media. 26
Figure 14: Modulated recording field. The sequence of magnetic fields applied to the triple-stack ML-3D media. The transitional external fields required to achieve the desired magnetic state were given 5 time units while 20 time units were designated for the final magnetic field. 26

Figure 15: Kerr rotation measurement. The simultaneous Kerr rotation produced by the ML-3D media as a result of the externally applied magnetic fields. The binary representation for each level along with its color coding are listed above each of the eight magnetic states. 27
Figure 16: AFM image of the triple-stack ML-3D BPM. 30
Figure 17: MFM image of the triple-stack ML-3D BPM. The MFM image corresponds directly to the nanopillars show in Figure 16. 30
Figure 18: Diagram of MFM data. A schematic highlighting the various magnetic states of the nanopillars shown in Figure 16. 32
Figure 19: Quantification of ML MFM signals. AFM/MFM section line analysis of the row of nanopillars located between the black arrows in Figure 17. The colored squares represent the different magnetic states as shown in Figure 10. The inset is a cropped section of the MFM image, taken between the two black arrows. 33
Figure 20: Quantification of ML MFM signals. AFM/MFM section line analysis of the row of nanopillars located between the red arrows in Figure 17. The color boxes represent the different magnetic states as shown in Figure 10. The inset is a cropped section of the MFM image, taken between the two red arrows. 33
Figure 21: Circuit diagrams and truth tables for (a) AND Gate, (b) OR Gate, (c) NOT Gate. 37
Figure 22: This shows the theoretical two layer media that exhibits 3 distinct levels of magnetization. 42
Figure 23: These graphs show the two clock pulses that are required to write the two input signals to the magnetic media. The third graph displays the output signal that is to read by the read head of the HDD. 44
Figure 24: Schematics of the EBL Process for BPM. 47
Figure 25: (a) AFM image of the patterned media, (b) MFM image of the patterned media, (c) Cross sectional view of the AFM (black) and MFM (blue) signals. 50
Figure 26: (a) AND, (b) OR gates of the three-layer reconfigurable magnetic logic gate. The direction of the magnetization determines if the bits is a 1 or a 0. “Up” = 1 and “Down” = 0. 55
Figure 27: A SEM image of 120 nm diameter patterns. 58
Figure 28: (a) Illustration of the direction of the magnetization of the probe with respect to the media, (b) An AFM image of the patterns that were used for the MFM study. The bits are 120 nm in diameter with different areal densities. 59
Figure 29: (a) AFM image, (b) MFM image of the 4 of the 8 possible input combinations, (c) An image created to highlight each of the individual four combinations with a different color and number, so that each one is easily distinguishable. 60
Figure 30: (a) AFM image, (b) MFM image of the other 4 possible input/reset combinations, (c) An image created to highlight each of the individual four combinations with a different color and number, so that each one is easily distinguishable. 62

Figure 31: (a) Two antiferromagnetically coupled adjacent cells to represent an inverter, NOT gate, (b) AND, (c) OR modes of a four-layer reconfigurable gate implementation. "Up" and "down" magnetization directions denote bits "1" and "0" respectively (↑= “1”, ↓= “0”). 66
Figure 32: An illustration (not to scale) of the 4-layer 3D media configuration 71
Figure 33: A Kerr-effect measured full M-H hysteresis loop. Minor loops are shown by different colors. The magnetic states in the four layers corresponding to different shoulders of the loop are coded as: AND/OR reset, IN B, IN A, and Output. 73

List of Tables

Table 1: Truth Table for the logic gates. 45
Table 2: Truth table for the reconfigurable AND/OR gate. 53
Table 3: Truth table for a reconfigurable AND/OR gate. AND and OR modes are determined by Reset = 1 and 0, respectively. The logic functions are defined by a code format (Input A, Input B, Reset, Output) as states on the hysteresis curve measured via magneto-optical Kerr effect. 70

Section 1 – Data Storage

Introduction

Presently, all magnetic-based data storage technologies are two-dimensional (2D) restricted. Conventional data storage devices store information in the form of 0′s and 1′s and are coded by the magnetization of ~35 nanoscale magnetic grains. The magnetization of these grains is oriented in either of two possible states and depends on the media predefined magnetic anisotropy axis. In this way, the recording and reading are done in a binary fashion from a single continuous magnetic layer. Increasing the areal density of data storage is achieved by writing more bits per track and more tracks per radial distance. Therefore, all the main components (reader/writer elements and magnetic media grain size) of a hard disk drive (HDD) must scale down in order to "squeeze" more information per unit area. Tremendous progress has been made for about five decades by scaling these components down. Nonetheless, in the past decade, the longitudinal magnetic recording (LMR) technology reached a fundamental (superparamagnetic) limit for areal densities between 100–200 $Gbit/in^2$ [1], [2].

The superparamagnetic limit occurs when thermal fluctuations in the media spontaneously switch the polarization of recorded bits within a relatively short time. This causes data loss and is an undesirable effect. The superparamagnetic limit is dependent upon the media grain size and magnetic anisotropy [3]. Hence, to defer this fundamental limit either higher anisotropy media or larger effective grain volume must be implemented. While the first requires relatively large switching magnetic field, the latter necessitates either thicker media or physical bit separation via patterning of the magnetic media.

To further increase the data storage capacity of HDDs, perpendicular magnetic recording (PMR) has been incorporated as a short-term solution. As the name suggests, bits are oriented in a perpendicular (out-of-plane) direction as opposed to the longitudinal (in-plane) direction. This enables magnetic recording on larger anisotropy magnetic media with greater grain volume [4]. As with LMR, limitations of PMR include media stability and read/write field. Since PMR is predicted to reach the superparamagnetic limit at ~1 Tbit/in^2, alternate technologies are vital to advance the magnetic-based storage technology and save it from becoming a mere commodity.

The two main proposed technologies under serious consideration are heat (or energy) assisted magnetic recording (HAMR) and bit patterned media (BPM). In the case of HAMR, a hybrid recording head is used to provide both heat and magnetic energy to switch the magnetization of ultrahigh anisotropy magnetic media [5], [6]. Main obstacles for this technology include allocation of a nanoscale heat spot with sufficient energy and fabrication of suitable magnetic media with sub-5 nm grain size [7], [8]. The BPM approach can defer the superparamagnetic limit by physically patterning the magnetic media [9]. Since the media is composed of exchange-coupled magnetic grains, the effective volume of a patterned bit is attributed to the volume of the bit as opposed to the volume of a single grain within a bit. Consequently, the bit becomes resilient to thermal fluctuations and the readback signal-to-noise ratio (SNR) increases as well. For fabrication, either direct patterning of the magnetic media or deposition of the magnetic composition on prepatterned media can be employed. Issues that must be addressed to achieve this technology include the mass production of patterned disks with bit separation below 25 nm and read/write position synchronization [10]. Regardless of the implementation level of either or both technologies, they are still 2-D limited. Eventually, multilevel (ML)-3D magnetic recording may be obligatory to further advance the progression of higher density magnetic storage [11], [12]. The focus of this section will be to first present a study of Co/Pd multilayers as a candidate material for a ML-3D magnetic recording. Following that, a three layer, bit-patterned, magnetic media that can be used for the next generation of ML-3D magnetic recording.

Study of Co/Pd Multilayers

Introduction

It is known that multilayer (ML) magnetic films consisting of laminated structures of Co/Pd pairs exhibit relatively high perpendicular magnetic anisotropy (PMA), whereas the thickness of each individual Co/Pd pair in the laminated stack can have a profound effect on the film's local magnetic properties [13], [14]. For instance, the alloylike nature is dominant at the interfaces and yields PMA through the strain anisotropy of Co atoms [15]–[19], while the thicknesses of Co and Pd layers within each local pair could be used to create vertical gradients of important local properties such as the magnetization and the coercivity field. In other words, a stack of Co/Pd MLs can be treated as a three-dimensional (3D) architecture with local properties tailored to specific applications. If necessary, we could also add Co/Pt MLs in the recipe to further expand the range of accessible properties. For instance, Co/Pd and Co/Pt MLs could be used to generate relatively high (2 to over 10 kOe) and relatively small (50 to over 1 kOe) coercivity values. However, in this particular study, with the goal to simplify the explanation, we will limit our- selves to using Co/Pd MLs only. Among important potential applications for the ML architectures under study are alternative magnetic recording modes such as heat-assisted magnetic recording, bit patterned media (BPM), exchange coupled composite media, and multilevel 3D (ML-3D) magnetic recording [4], [12], [20], [21]. Moreover, recently, magnetic logic devices were proposed as alternatives to conventional silicon semiconductor logic technologies [22], [23]. These new computer processing units could also benefit from the use of the 3D architecture of the ML media under study [24].

In this section, we will present a study to use a combinatorial synthesis to tailor magnetic properties of 3D Co/Pd ML media to specific applications such as the above magnetic technologies and potentially other magnetic applications of the future.

Experiment

Co/Pd ML thin films were sputter-deposited on Si (100) substrates in a magnetron sputtering system AJA Orion 5. The base pressure in the chamber was maintained below 10^{-7} Torr. The deposition was performed at room temperature. Direct current power values of 56.25 and 18.75 W were applied for the Co and Pd target deposition, respectively. The sputtering rates for the 5 mTorr processing pressure were measured to be 0.39 Å/s and 0.41 Å/s for Co and Pd, respectively. Following the deposition of the 5-nm-thick Pd seed layer, a stack of *n* Co (0.26 nm)/Pd (0.5 nm) pairs (bilayers) was deposited. The composition of the film was finely controlled by adjusting the thicknesses of Co and Pd layers. In this fabrication process, the MLs were deposited from two angled guns onto a rotating substrate. The substrate rotation was maintained at approximately 30 rpm.

The surface topography of thin films under study was measured with the atomic force microscopy (AFM) mode of a DI's scanning probe microscopy system Dimension 3100. The magnetic force microscopy (MFM) mode was used to observe magnetic domains in demagnetized samples. A focused magneto-optical Kerr effect (F-MOKE) system was used to measure the magnetic hysteresis loops of the new structures.

Results and Discussion

A. Effect of substrate argon ion milling

Since the key properties of the ML structures are surface induced, it was not unnatural to explore the effect of Ar^+ milling on the magnetic properties. Ar^+ milling was performed on the substrates prior to the deposition of the MLs themselves. The milling was performed with radio frequency power of 12.5 W under pressure of 5 mTorr for 2 min. The original purpose of Ar^+ milling was to remove the native silicon-oxide and relatively small particles from the substrate surface. The AFM analysis of the silicon substrate before and after Ar^+ milling indicated that the milling improved the surface roughness by more than a factor, as shown in Figure 1. A composition of Pd(5 nm)/[Co(0.3 nm)/Pd(0.5 nm)]$_7$/Pd(5 nm) was then sputter-deposited on Ar^+ milled and "as is" silicon substrates. Figure 1(c) shows a comparison between the hysteresis loops of Co/Pd MLs on Si substrates prior and after Ar^+ milling. It can be observed that Ar^+ milling increased the coercivity to over 2.23 kOe, i.e., by a factor of 3 compared to that for the media deposited on the "as is" substrate, i.e., approximately 788 Oe. It is possible that the removal of the native SiO_2 layer and the consequent deposition on a relatively smooth crystalline Si surface resulted in improved crystallographic growth, which in turn was shown to increase the coercivity of Co/Pd MLs [25], [26]. Therefore, smoother surface and lower roughness substrates were found to be advantageous to the growth of higher coercivity Co/Pd MLs. Due to the significant improvement in the media's coercivity, all further samples were sputter-deposited on Ar^+-milled Si substrates.

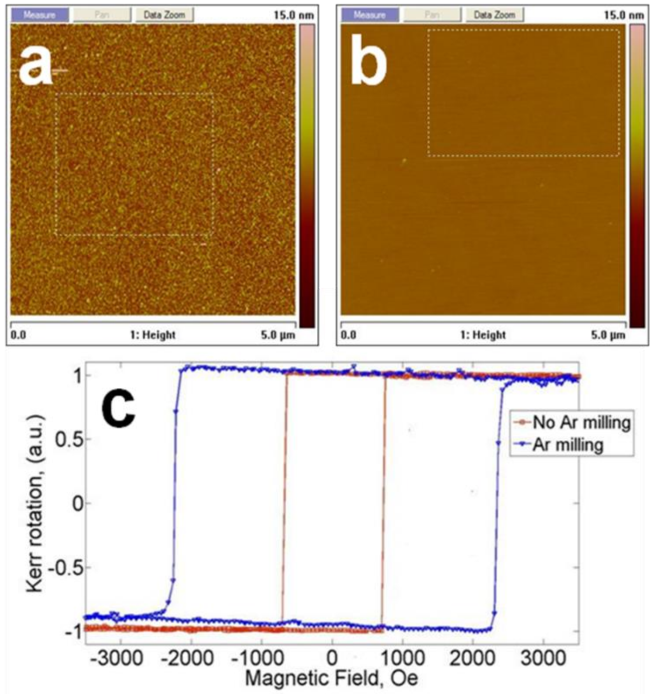

Figure 1: AFM images (5 X 5 µm^2) of a Si substrate (a) prior to Ar^+ milling, (b) after Ar^+ milling with roughness (Ra) values of 0.791 nm and 0.077 nm, respectively. The roughness measurements were taken from the high-lighted rectangular frames, (c) A comparison of hysteresis loops for Co/Pd MLs deposited on Si substrates with and without Ar^+ milling.

B. Coercivity dependence on Co and Pd thickness

It is known that the properties of Co/Pd MLs can be significantly controlled by adjusting the thickness values for Pd and Co layers [27]. A series of Pd (5 nm)/[Co(x nm)/Pd(0.55 nm)]$_7$/Pd(5 nm) ML films with a fixed Pd layer thickness of 0.55 nm were grown on Si substrates. The thickness of Co layer, x, was varied from 0.15 to 0.45 nm.

Hysteresis loops were measured with an F-MOKE system as shown in Figure 2. We found that the coercivity began to decrease when the thickness of Co layer was increased over ~0.26 nm (Figure 3). This effect might be due to the increase in the demagnetization field as a consequence of higher Co concentration. A similar series of Pd(5 nm)/[Co(0.26 nm)/Pd(*y* nm)]$_{7/}$Pd(5 nm) multilayered samples was prepared on a Si substrate at room temperature. The thickness of the Pd layer, *y*, was varied from 0.5 to 0.6 nm. The measurements indicated that a Pd layer thickness of 0.55 nm produced the highest coercivity on Si, as shown in Figure 4.

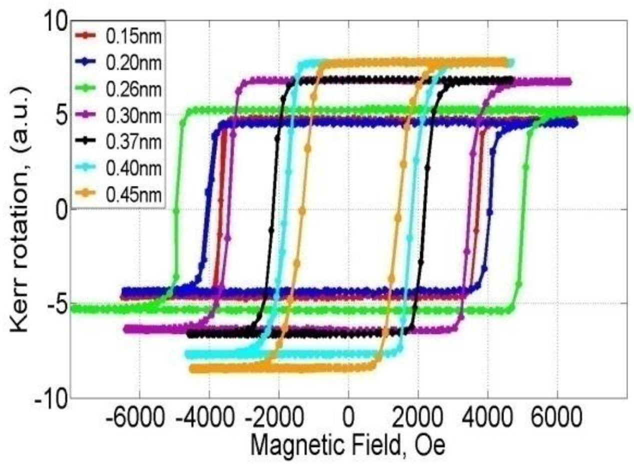

Figure 2: Hysteresis loops of Co/Pd MLs on Si substrate with the variance of Co bilayer thickness.

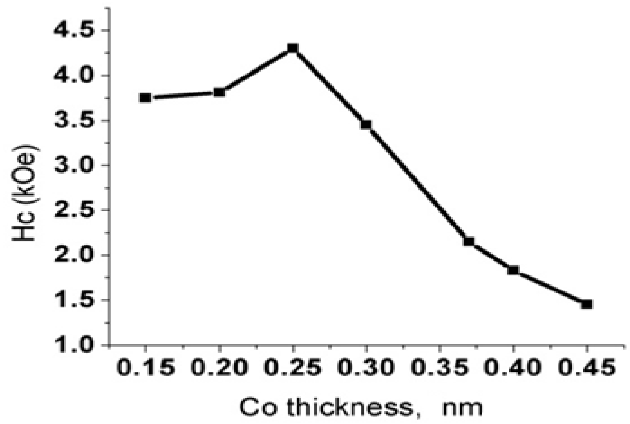

Figure 3: Coercivity behavior of Co/Pd MLs on Si substrate as a function of Co-bilayer thickness.

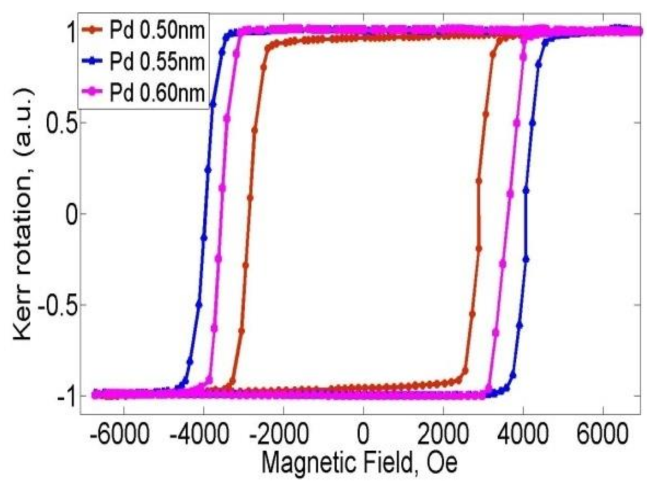

Figure 4: Hysteresis loops of Pd(5 nm)/[Co(0.26 nm)/Pd(y nm)]$_7$/Pd(5 nm) on Si substrate with the variance of Pd bilayer thickness.

C. Deposition pressure versus coercivity

We prepared a series of Pd(5 nm)/[Co(0.26 nm)/Pd(0.55 nm)]$_{7}$/Pd(5 nm) Co/Pd MLs with different processing pressures. The deposition pressures for the Co/Pd MLs were 5 mTorr and 15 mTorr, while the pressure during the seed and capping layers deposition was always maintained at 5 mTorr. Figure 5 shows the comparison of the hysteresis loops of Co/Pd MLs at different processing pressures. It can be observed that the coercivity increased from approximately 4.89 to over 5.69 kOe as the processing pressure was raised from 5 to 15 mTorr.

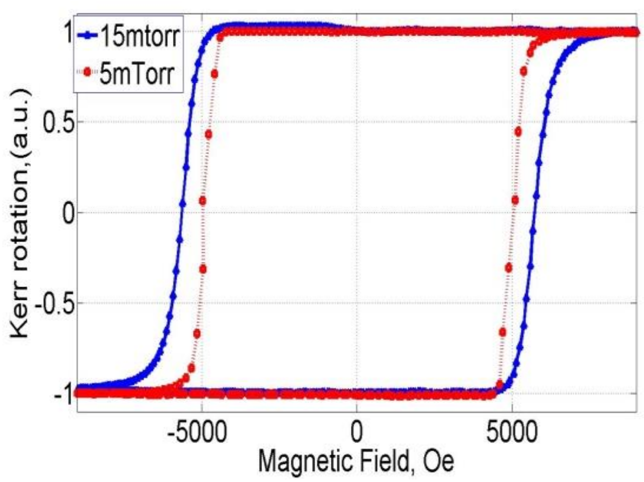

Figure 5: Hysteresis loops of Co/Pd MLs deposited at different processing pressures.

The intergranular magnetic exchange coupling parameter α provides a measure of the magnetic exchange interaction strength between the grains in the film. The steeper the loop shoulders, the stronger the exchange interaction between the grains. The decoupling of the grains, which results in higher coercivity, is attributed to the grain segregation with higher processing pressure. The hysteresis loop shoulders tend to roll over more continuously with higher pressure, which suggests that the grains are becoming segregated and weakly coupled, magnetically, or even exchange-decoupled.

Figure 6 shows MFM images of ac demagnetized samples for which the hysteresis curves are shown in Figure 5. A correlation may be drawn between the intergranular exchange and the size of the magnetic domains/clusters. Relatively large magnetic clusters are generated for stack ML media that was deposited at a lower processing pressure, as shown in Figure 6(a). This type of media can be suitable for BPM as suggested by both the hysteresis measurement and MFM analysis. For the same reason, a higher processing pressure is favorable for the formation of granular media. It can be seen that the magnetic domains are substantially reduced when sputtered at a higher pressure, as shown in Figure 6(b). The kinetic energy of atoms and clusters is reduced with higher Ar^+ pressure, thus the growth of Co/Pd MLs is dominated by a nucleation mechanism, which results in more segregated grains. The higher processing pressure can therefore be utilized to promote more segregated magnetic grains and may be applied to fabricate a granular media. The maximum domain size for the samples deposited at 5 mTorr and 15 mTorr were calculated to be 6.0 μm^2 and 1.3 μm^2, respectively. In summary, Co/Pd MLs media can be tailored to exhibit either exchanged-coupled or exchange-decoupled magnetic grains, which are suitable for either BPM or granular media, respectively.

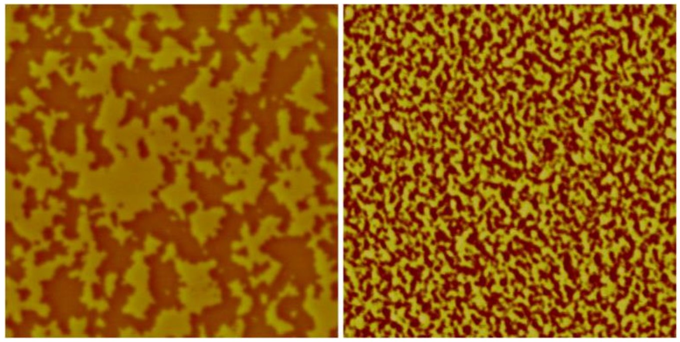

Figure 6: MFM images (5 X 5 μm^2) of demagnetized samples with different processing pressure on Si substrate (a) 5 mTorr, (b) 15 mTorr.

D. Number of MLs versus coercivity

We sputter-deposited a series of Pd(5 nm)/[Co(0.26 nm)/Pd(0.55 nm)]$_n$/Pd(5.3 nm), where *n* is the number of layers in the stack, at room temperature and a processing pressure of 5 mTorr. The results revealed that the highest coercivity was observed when *n* equaled 7 b Co/Pd pairs, followed by a sharp decline in the coercivity, as illustrated in Figure 7. The relationship between the coercivity and the number of Co/Pd pairs was thus not linear. Rozatian *et al.* suggested that the loss of conformity was the cause of the reduction in the anisotropy energy per interface as the number of ML pairs increased [28].

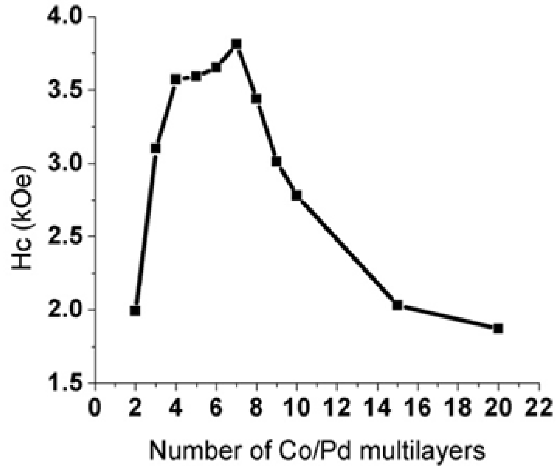

Figure 7: Coercivity behavior of Co/Pd MLs as a function of the number of Co/Pd MLs (n).

E. ML-3D magnetic recording media

The concept of ML-3D magnetic recording media as a next generation recording technology has been previously proposed [12]. By stacking recording layers in a third dimension we could effectively increase the areal density of magnetic storage beyond 10 Tbits/in.^{2}. Co/Pd MLs exhibiting relatively high perpendicular anisotropy is a promising candidate for ML-3D magnetic recording media. As illustrated in Figure 7, when *n* equaled 2, the coercivity of Co/Pd MLs in the current study was approximately 1.99 kOe. When *n* equaled 7, the Co/Pd MLs provided the highest coercivity of approximately 3.98 kOe. When *n* equaled 10, the coercivity was in the middle between the highest and the lowest values. From the above results, 2, 7, and 10 were chosen to fabricate a three-stack Co/Pd ML magnetic recording media. The composition of the resultant three stack ML media was the following: substrate/Pd(5 nm)/[Co(0.26 nm)/Pd(0.55 nm)]$_{10}$/Pd(5 nm)/[Co(0.26 nm)/Pd(0.55 nm)]$_7$/Pd(5 nm)/[Co(0.26 nm)/Pd(0.55 nm)]$_2$/Pd(5.3 nm). [Co(0.26 nm)/Pd(0.55 nm)]$_n$ acts like one "single" magnetic layer. Here, the non-magnetic material Pd(5 nm) was used as an interlayer to break the exchange coupling between adjacent magnetic layers and thus to independently record information into the three layers.

The three-stack Co/Pd MLs media was saturated by adding a relatively large magnetic field to fully utilize the hysteresis loop with three plateaus, as shown in Figure 8. The directions of the magnetization are marked by arrows to reflect the eight signal levels generated by the three-stack multilevel recording media. MFM images of each separate stack and the combined triple stack are presented in Figure 9. Before the measurements, all the samples were first demagnetized by applying an alternating decaying magnetic field. All the samples were scanned with the same MFM probe and at the same scanning parameters in order to detect minute signal differences between the four ML media types under study. As illustrated in the figure, multiple signal levels were evident for the three-stack media.

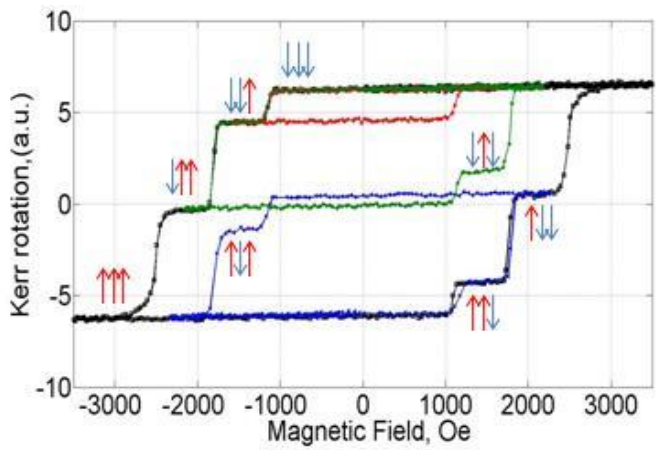

Figure 8: Major and minor hysteresis loops of three stack Co/Pd MLs on silicon substrate.

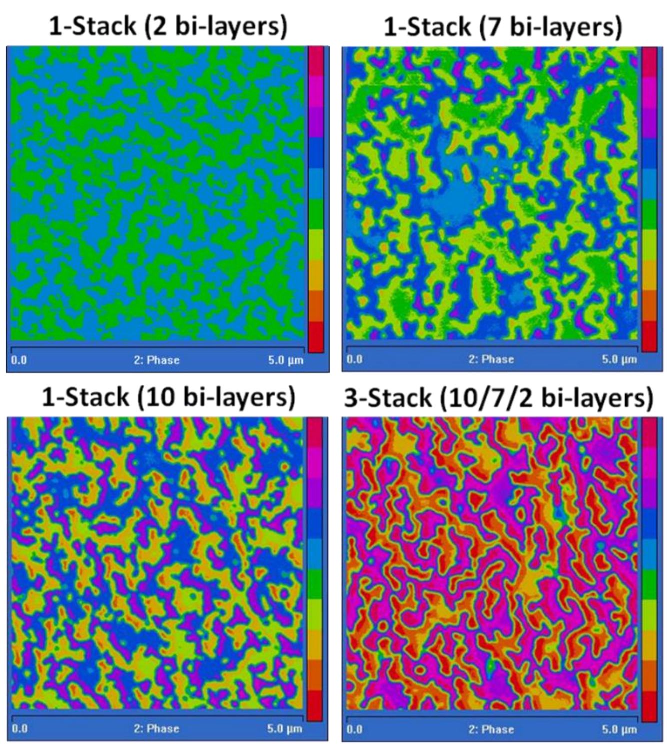

Figure 9: MFM images (5 X 5 µm^2) of single-stack Co/Pd MLs media for two, seven, and ten bilayers and a triple-stack Co/Pd MLs media exhibiting all three layers together, starting with the ten bilayers stack in the bottom and the two bilayers stack at the top.

Conclusion

In summary, the effect of substrate argon ion milling, the variance of Co and Pd layer thicknesses, the number of Co/Pd pairs, and the processing pressure were analyzed to produce Co/Pd MLs with the highest possible range of the coercivity and the highest possible remanent squareness. Substrate Ar^+ milling was effective to achieve the high coercivity magnetic media. The variance of Co and Pd layer thicknesses was also studied. For granular media applications, higher processing pressure was found to favor the granular structure of Co/Pd MLs. On the contrary, it was found that lower processing pressure could be used to generate exchange-coupled magnetic grains, which was suitable for BPM and nanomagnetic logic systems. The relation between the number of Co/Pd pairs and the coercivity was not linear and therefore might be used to fabricate ML-3D magnetic recording media. Three stack Co/Pd MLs which could generate up to eight signal levels were fabricated by sputtering Co/Pd MLs.

The results found in this section will be used as the building blocks for the rest of the research described in the following sections. First, these results are used to fabricate a tri-layer patterned magnetic media for data storage applications. This was done first, because the operation of the media for data storage is easier than logic operations. Once it was verified that the media could be used for data storage, then research into using Co/Pd based media for data storage could be conducted.

* Some of the material presented in this chapter was reprinted with permission from B. Hu, et al., *J. Appl. Phys.*, vol. 109, no. 3, p. 034314, Feb. 2011.

Multilevel-3D Bit Patterned Magnetic Media with 8 Signal Levels per Nanocolumn

Introduction

In ML-3D magnetic recording, at least two magnetic layers ($N \geq 2$) are used to both read and write information. The ML readback signal is proportional to the vector sum of the magnetic fields generated by the N magnetic layers. Amplitude detection of the playback signal is thus required to distinguish the various signal levels. Such detection mechanism has been implemented previously in ML optical storage [29], [30]. Assuming an ideal case where each layer generates two readable and distinguishable signal levels, the effective areal density increases by a factor of N. To selectively write on N layers, the ML-3D magnetic media must exhibit a variation in magnetic properties across its thickness. One option is to create a coercivity (H_{cN}) gradient, where individual magnetic layers are accessed by changing the magnitude and direction of the write field. Finally, integrating the ML-3D approach with BPM may also relax the patterning constraints while still increasing the capacity of data storage devices. This is because the effective information density becomes a function of the number of signal levels that can be accessed as well as the distance between individual bits.

To date, both industry and academic institutions have shown growing interest in ML-3D magnetic recording [31]–[34]. Feasibility work has been presented on dual-layer Co/Pd and dual-layer Co/Pt multilayers [35], [36]. The main concern under consideration was the ferromagnetic coupling between multilayers stacks of Co/Pd-Co/Pd and Co/Pt-Co/Pt dual-stack media [37]. It was shown that opposing poles were not the preferred demagnetization state for these types of media. Alternate magnetic dual-layer media using oblique evaporated Co-CoO medium has also been proposed as a method of recording on more than one layer [38]. Finally, implementation of microwave assisted magnetic recording was also considered for dual-layer ML-3D recording [39], [40].

Arguably, the most important challenges with addressing more than one magnetic layer can be summarized as the following three problems. First, the recording field is weaker at larger distances from the recording head. Therefore, a limitation exists on the total number of independent magnetic layers that can be stacked across the media. In order for a bit of information to be recorded, the magnetic field should overcome the coercivity of the media in the region of the bit. Second, it is a challenge to selectively write on each layer due to the relatively strong ferromagnetic interaction between adjacent layers. Third, it is not trivial to distinguish the magnetic state of individual magnetic layers during the playback process because of the superposition of all the fields emanating from different layers. To address these challenges and demonstrate the feasibility of a ML-3D recording system, we have studied hybrid ML-3D media that is composed of both Co/Pd and Co/Pt multilayers. In this letter, we reveal the results of triple-stack (Substrate)-Co/Pt-Co/Pd-Co/Pd ML-3D BPM. The analysis of this media highlights our findings and signifies the combination of Co/Pd and Co/Pt multilayers in the first generation ML-3D BPM.

We exploit exchange-coupled Co/Pd and Co/Pt multilayers, which due to their relatively high perpendicular magnetic anisotropy are being considered for PMR and BPM [19], [41]. The structure of multilayers media is composed of a stack of Co/Pt or Co/Pd pairs, where the thickness of each pair is commonly below ~2 nm. Because of the relatively thin Pd or Pt thickness, the pairs within a single stack of multilayers are exchange-coupled. Consequently, each multilayers stack is considered to be a single magnetic layer. To isolate adjacent stacks for ML-3D magnetic recording, a relatively thick non-magnetic composition is inserted between the stacks.

To effectively fabricate ML-3D media, we amalgamate Co/Pd and Co/Pt multilayers to provide a substantially wider range of key properties, such as coercivity (H_c) and saturation magnetization (M_s). These properties can be controlled via the deposition parameters, selected compounds, thickness of each element within a pair, and the number of pairs within a stack [42]. For this study, a combinatorial synthesis process has been implemented to achieve material compositions necessary to control gradients of coercivity and magnetic moment (m_N) across the thickness of ML-3D media. Varying the magnetic moment across the recording media makes it possible to distinguish different stacks from each other during the readback process. The M_s and thickness of each stack define its total magnetic moment. In summary, we formulated the following rule of thumb to define relationships between the magnetic properties of different magnetic layers: $m_1 \geq 2m_2 \geq 4m_3 \geq 2^{N-1}m_N$ and $H_{cN} > H_{c3} > H_{c2} > H_{c1}$, where$m_1$ and H_{c1} are the total magnetic moment and coercivity of the bottommost layer. *Figure 10* shows a schematic representation of the media structure and preferred magnetic properties. The attainable magnetic states and their binary and color notations are illustrated as well.

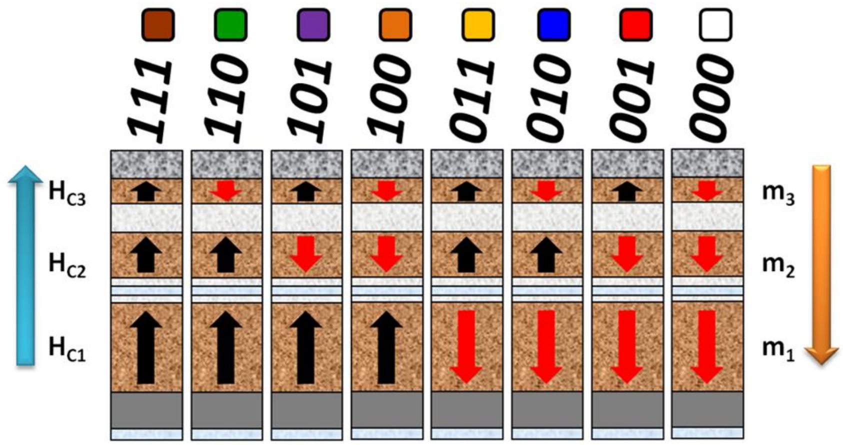

Figure 10: Triple-stack ML-3D BPM. Schematic of the structure and desired magnetic properties (not to scale). The black arrows (binary "1″) and red arrows (binary "0″) denote the two possible magnetic states in each stack. Above the columns lies the binary representation and color coding for the eight possible magnetic states.

Materials and Methods

A. Homogeneous ML-3D Media Fabrication

The surface properties of a Si (100) substrate were modified in order to optimize the magnetic properties of the ML-3D media. This was done by Ar-ion milling the native SiO_2 on the surface of the substrate prior to deposition. A selected composition of (Substrate)-Ti(1.5 nm)/Pt(5 nm)/[Co(0.4 nm)/Pt(0.55 nm)]×14/Pt(1.5 nm)/Ti(1.5 nm)/Pd(1.5 nm)/[Co(0.25 nm)/Pd(0.55 nm)]×7/Pd(4.5 nm)/[Co(0.25 nm)/Pd(0.55 nm)]×3/Pd(3 nm)/Ti(4 nm) was then sputter-deposited on the substrate, Figure 11. This composition was nominated to both demonstrate the feasibility of effectively storing magnetic information in a 3rd dimension and enable MFM imaging of all the readback levels with acceptable SNR. For the presented ML-3D media, the effective magnetic moment in each strongly coupled multilayers stack was closely proportional to the total Co thickness in each layer. This was determined from a vibrating-sample-magnetometer (VSM) measurement. To ensure adequate decoupling between adjacent magnetic layers, we maintained an isolation thickness of ~5 nm. The Ti interlayer (1.5 nm) between the Co/Pt and first Co/Pd multilayers stacks promoted exchange-coupled grains within the Co/Pd multilayers stacks. Following the deposition process, the media was placed in ambient conditions to induce the natural oxidation of the Ti capping layer. The oxidized Ti layer served as an HSQ adhesion layer as well as a hard-mask for the pattern transfer process, e.g. from HSQ nanoscale patterns to ML-3D magnetic nanopillars.

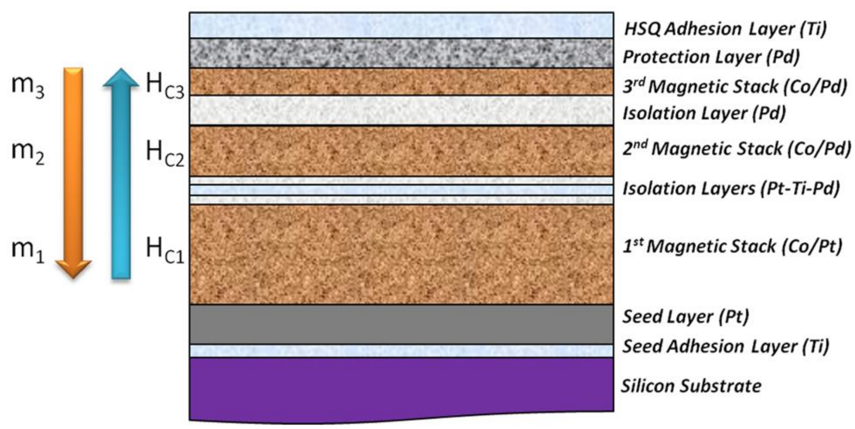

Figure 11: ML-3D magnetic media composition.

B. Patterned ML-3D Media Fabrication

Electron-beam lithography (EBL) was used to fabricate arrays of periodic hydrogen silsesquioxane (HSQ) nanoscale patterns on the surface of the above described triple-stack ML-3D media. First, diluted HSQ and Methyl isobutyl ketone (MIBK) 1:2.5 were spin-coated on the ML-3D magnetic media, followed by heat treatment at ~140°C, Figure 12(b). Second, the patterns were exposed by a JEOL direct-write EBL system (JBX-5500FS) using 50 keV beam intensity, 98 pA beam current, and an average dose of 3000 $\mu C/cm^2$. The sample was then developed in a MICROPOSIT™ MF™ CD-26 solution to uncover the electron-beam exposed HSQ patterns, Figure 12(c). The morphology and height of the developed patterns were confirmed with scanning electron microscopy (SEM) and AFM, respectively. A total of ~30 nm was measured for the final thickness of the developed HSQ patterns. Implementation of the above process produced HSQ features below 10 nm in diameters with separation distance of ~26 nm.

The procedure of transferring the HSQ patterns into the media necessitated a couple of steps. First, we exposed the sample to inductively-coupled plasma (ICP) reactive etching using a gas mixture of SF_6/Ar (50:50) at ~450 W for 30 seconds. The bare oxidized Ti layer was removed from around the HSQ patterns during this process. Second, the ICP power dropped to ~250 W and the SF_6 source closed, leaving only Ar gas in the chamber. This resulted in Ar-ion milling (or sputtering) of the HSQ patterns and ML-3D composition, which continued for an additional six minutes, Figure 12(e). The Ar-ion milling parameters were set to virtually not affect the oxidized Ti layer. Finally, confirmation of the transferred patterns was done through SEM and AFM imaging.

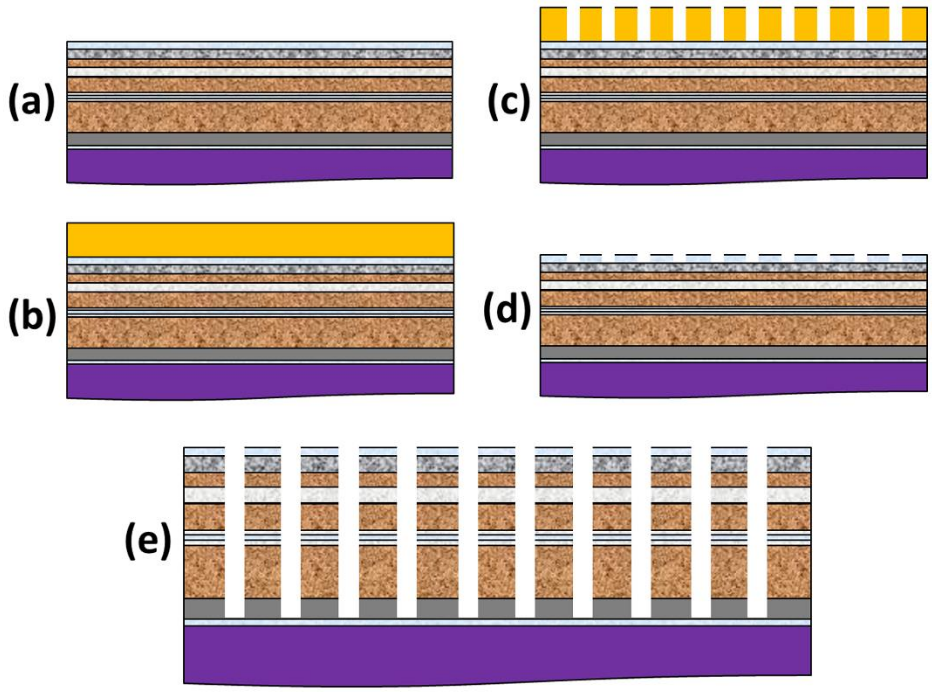

Figure 12: ML-3D BPM media fabrication process. (a) Sputter-deposition of the triple-stack ML-3D magnetic media composition, (b) Spin-coat and bake HSQ, (c) E-beam lithography (expose and develop patterns), (d) ICP etching of the naturally oxidized Ti layer, (e) Ar-ion milling of the remaining composition to form the triple-stack ML-3D BPM.

C. Magnetic Writing and Reading via Magnetic Force Microscopy

High resolution MFM probes with relatively high M_s, magnetic moment, and coercivity were custom designed and fabricated by Paramount Sensors LLC for this project. These probes were used to both write and read from the ML-3D BPM. To facilitate adequate writing and reading, these probes needed to exhibit a range of magnetic fields. Strong fields were needed to magnetize the media for writing while weaker fields were required to ensure no significant magnetic switching occurred during the MFM reading process. Fabricating the probes with a range of different protective coating thicknesses accomplished this. The probes with the thinner protective coating produced the highest magnetic field in the vicinity of the tip and were used to switch the magnetization of the Co/Pt stack in selected nanopillars. On the other hand, the probes with the relatively thicker protective coating emanated weaker magnetic fields and were utilized to read the recorded information. MFM imaging of the nanopillars was implemented using the *Lift Mode*™ technique with a tip-sample separation of ~20 nm.

Results and Discussion

A. Homogeneous ML-3D Media

The out-of-plane hysteresis loop for the entire ML-3D media composition is shown in Figure 12. Measurements of the curve were taken using a custom-built polar magneto-optical Kerr effect (P-MOKE) system. The discontinuous shape of the resulting hysteresis loop proves that the three stacks (each being a set of strongly coupled multilayers) are exchange-decoupled from each other. Also evident from this loop, are the magnetic moment and coercivity gradients. This means that the three magnetic layers (stacks) can be separated from each other during write and read operations. Furthermore, a careful inspection of the hysteresis curve reveals that the bottommost (Co/Pt) and topmost (Co/Pd) layers produced Kerr signals which are relatively lower and higher when compared to the total Co thickness in each layer, respectively. This is the result of light transmission/reflection from the triple-stack media. The MFM interaction with the triple-stack media can thus be approximated from the hysteresis measurement. In MFM analysis, the proximity of the magnetic tip with respect to each magnetic layer will produce a similar outcome.

To write 8-level information in the triple-stack ML-3D media, we take advantage of the knowledge stored in the hysteresis loop. The full hysteresis loop is defined as the reaction of the magnetization to continuous variation of externally applied magnetic field, from $+\infty$ to $-\infty$ and back to $+\infty$. Using the full loop ensures a predictable way to record six of the eight signal levels (i.e. 111, 011, 001, 000, 100, and 110) in no more than two steps, Figure 13. To record these six levels, the ML-3D media is magnetized in a certain order according to the full loop. For example, to achieve the signal level "011", a large positive recording field is applied as the first step to saturate the media in "111" direction, and as the second step, the field is reversed to the value sufficient to reach the desired magnetic state. In the same way, any other of the six states can be reached. To attain the two remaining states (101 and 010), it is necessary to use minor hysteresis loops and thus three steps to perform the recording. To initiate a minor hysteresis loop, a field reversal has to be initiated before the full loop is closed. Figure 14 and Figure 15 show how all eight levels can be recorded (via externally applied magnetic fields) and simultaneously read (via the P-MOKE) from the triple-stack ML-3D media, respectively. The short time slots reflect transitional external fields which are applied to achieve the desired magnetic state. The longer time periods indicate the final externally applied magnetic field to achieve each of the eight magnetic states.

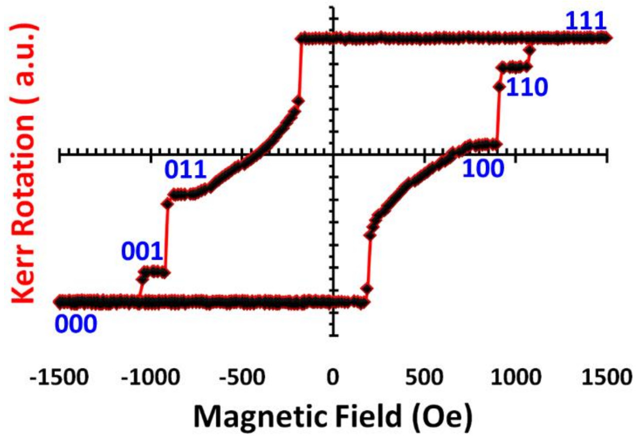

Figure 13: MOKE hysteresis loop. A graph revealing three magnetically-decoupled recording layers for the fabricated ML-3D media.

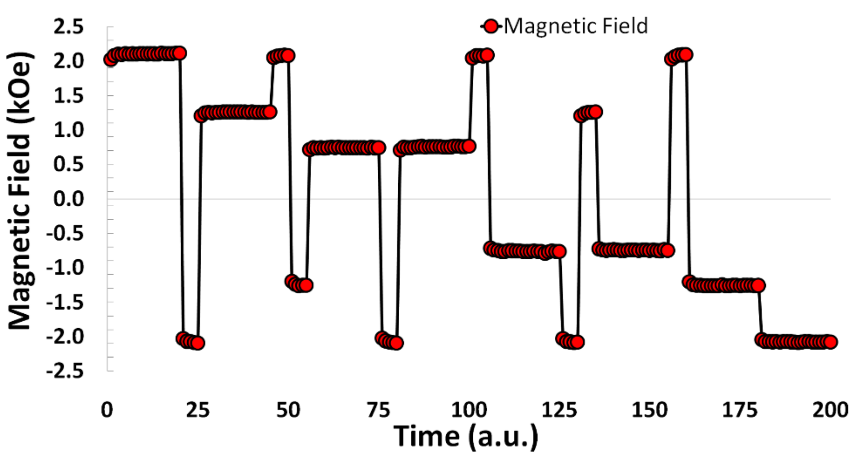

Figure 14: Modulated recording field. The sequence of magnetic fields applied to the triple-stack ML-3D media. The transitional external fields required to achieve the desired magnetic state were given 5 time units while 20 time units were designated for the final magnetic field.

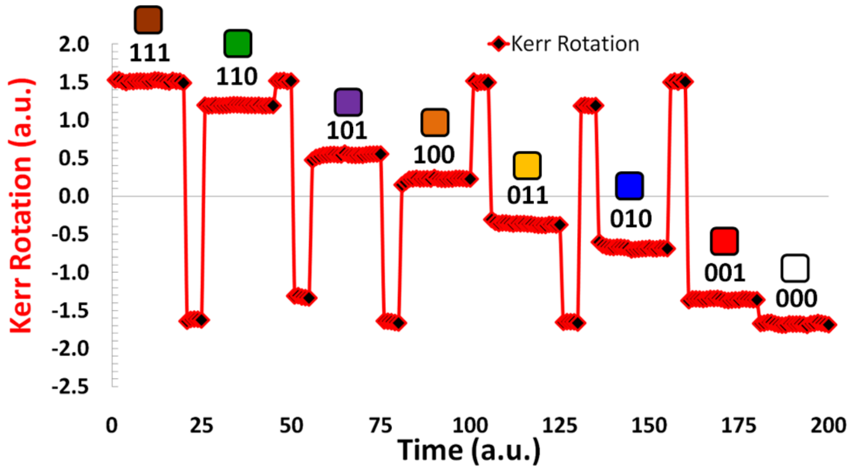

Figure 15: Kerr rotation measurement. The simultaneous Kerr rotation produced by the ML-3D media as a result of the externally applied magnetic fields. The binary representation for each level along with its color coding are listed above each of the eight magnetic states.

B. Patterned ML-3D Media

The ML-3D BPM was initially demagnetized to investigate the preferred magnetic energy state of the nanopillars. To perform this analysis, the sample was exposed to an alternating and decaying magnetic field, starting at ~7,500 Oe and ending at ~1 Oe. The magnetic field alternated along the easy axis of the magnetic media (out-of-plane direction). We then analyzed the demagnetized media by performing MFM imaging on arrays of nanopillars. The MFM data showed that more than 97% of the nanopillars were in a partially antiferromagnetic state (e.g. 100 or 011 states). These results revealed that for this particular ML-3D BPM, the stored information across each nanopillar would be stable for at least two states with undesirable (antiferromagnetic) orientations.

Ideally, a nanoscale electromagnetic transducer would have been used to selectively write on each layer of each nanopillar by locally varying the magnitude and direction of the write field. In the present case, we configured the ML-3D BPM to exhibit 8-level magnetic information by further exposing it to a series of externally applied magnetic fields. To start with, a magnetic field of ~17,000 Oe was applied along the magnetic hard axis (in-plane direction) of the media. Applying this field facilitated partial recording of the antiferromagnetic states between the two Co/Pd stacks (e.g. X01 and X10, where "X" represents the magnetic state of the bottommost Co/Pt layer which may either be a "0" or a "1"). Approximately 13% of the analyzed nanopillars changed their magnetic states from "X00" or "X11" to "X01" or "X10". At this stage, the four possible magnetic states (e.g. X11, X00, X01, and X10) for the two Co/Pd stacks were locked in place. Randomizing the magnetic state of the third Co/Pt stack would finalize the recording of all eight levels. This could be done without modifying the previously recorded states in the Co/Pd stacks since the switching field for the Co/Pt stack was less than the coercivity fields of the Co/Pd stacks. First, we applied a magnetic field of ~3,000 Oe along the magnetic easy axis of the media. This field caused the magnetic state of the Co/Pt stack in each nanopillar to be in the "0" state. Next, an MFM probe with the thinnest protective coating was magnetized in such a way that when used to AFM-scan the nanopillars, the magnetization of the Co/Pt stack in each nanopillar would switch its state from "0" to "1". The set of patterns on the right-side of Figure 16 was AFM-scanned with this MFM probe. Finally, the eight magnetic states of the ML-3D BPM could be simultaneously revealed by taking an MFM image of both sets of patterns.

Magnetic force microscopy imaging of the nanopillars shown in Figure 16 was taken using an MFM probe with relatively thicker protective coating. Prior to imaging, the probe was magnetized along the tip central axis and into the tip (in the “1” direction with respect to the media). This probe caused the Co/Pt stack of only several nanopillars to switch its magnetic state from “0” to “1” during the initial scan of the patterns. Therefore, the protective coating thickness for this particular probe proved sufficient to enable the MFM reading of the final magnetic states.

The MFM image shown in Figure 17 was captured after a few scans of the same sets of patterns. The darker and lighter colors of the image-scale indicate the level of long-range magnetostatic attraction and repulsion between the tip and media, respectively. Therefore, the nanopillars that generated the lowest MFM signal (dark brown) were in the “111” state, while the ones that produced the highest signal (bright yellow) were in the “000” state. An assessment of the left-side set of patterns indicated that the globally applied magnetic field of ~3,000 Oe switched the magnetization of the Co/Pt stack to the “0” state. It also showed the location of the nanopillars that had their magnetic state modified in the first MFM scan. The results for the patterns on the right-side revealed that the MFM probe with the thinnest protective layer generated strong enough magnetic field to change the magnetic state of the bottommost layer in more than 97% of the nanopillars.

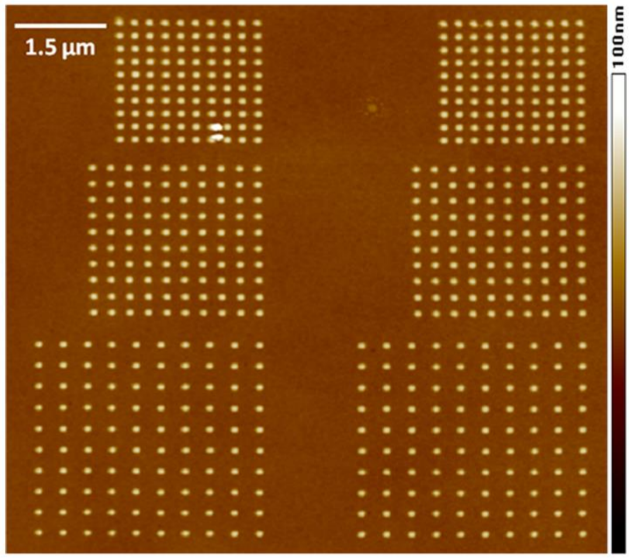

Figure 16: AFM image of the triple-stack ML-3D BPM.

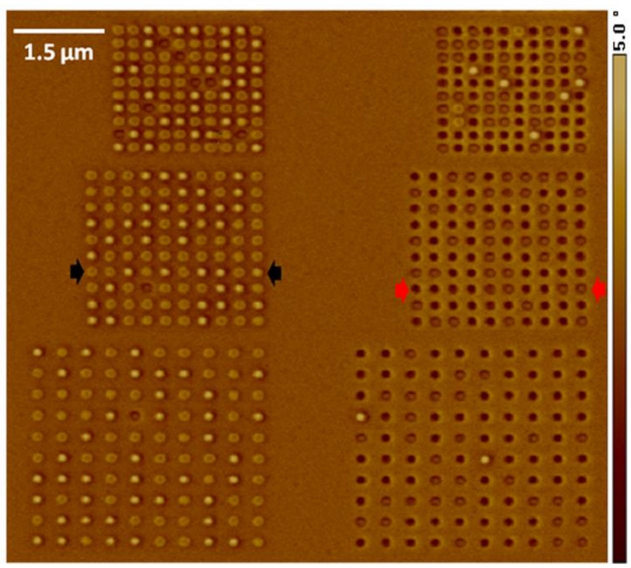

Figure 17: MFM image of the triple-stack ML-3D BPM. The MFM image corresponds directly to the nanopillars show in Figure 16.

A detailed examination of Figure 17 exposed all the possible magnetic states for the triple-stack ML-3D BPM. To highlight the various magnetic signal levels, we examined the MFM signal produced by each nanopillar and created a diagram representation for the MFM image, Figure 18. These states were quantified by performing AFM/MFM section line analysis across the central points of the nanopillars. Figure 19 and Figure 20 are examples of section line investigations, which were performed for the rows of nanopillars located between the black and red arrows in Figure 17, respectively. As is evident from the diagram and section line investigations, the triple-stack ML-3D BPM produced eight discrete magnetic states.

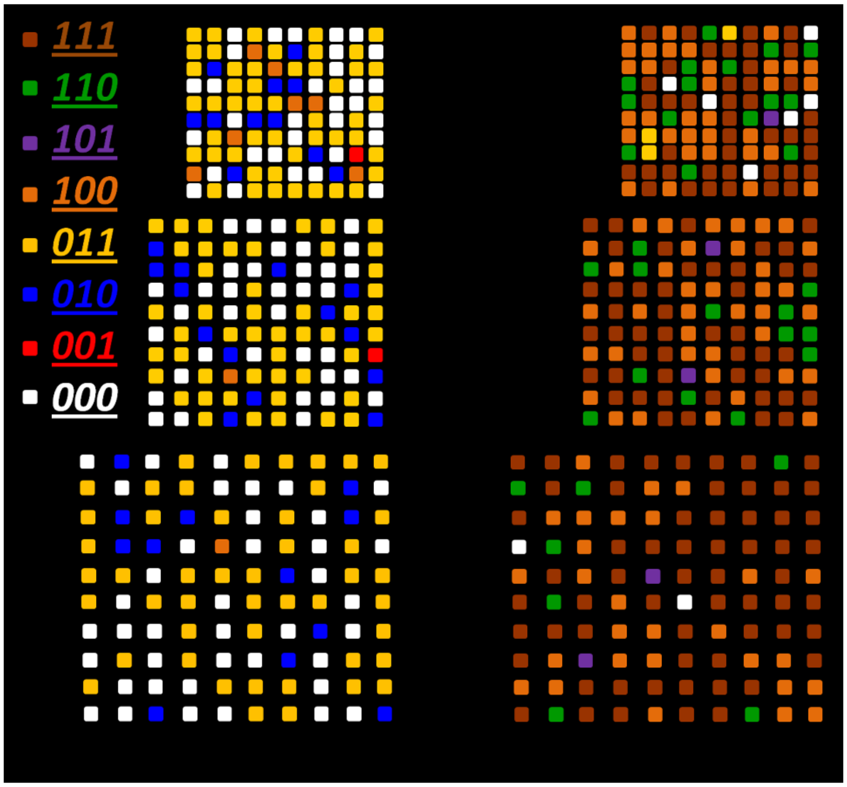

Figure 18: Diagram of MFM data. A schematic highlighting the various magnetic states of the nanopillars shown in Figure 16.

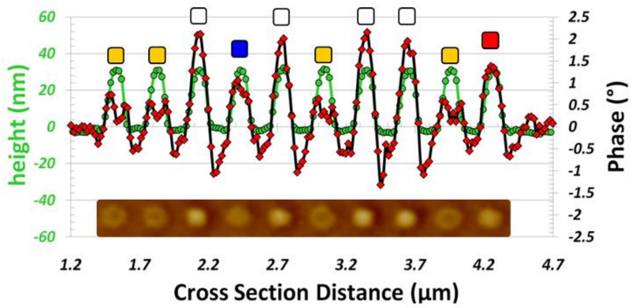

Figure 19: Quantification of ML MFM signals. AFM/MFM section line analysis of the row of nanopillars located between the black arrows in Figure 17. The colored squares represent the different magnetic states as shown in Figure 10. The inset is a cropped section of the MFM image, taken between the two black arrows.

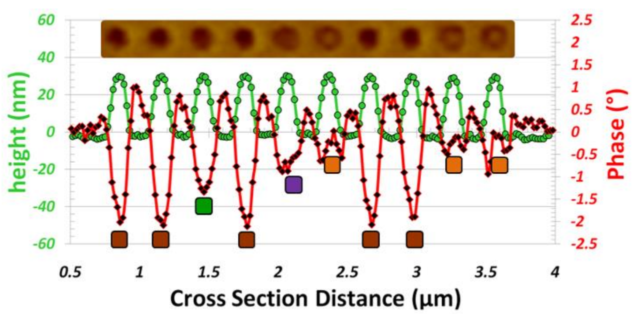

Figure 20: Quantification of ML MFM signals. AFM/MFM section line analysis of the row of nanopillars located between the red arrows in Figure 17. The color boxes represent the different magnetic states as shown in Figure 10. The inset is a cropped section of the MFM image, taken between the two red arrows.

Conclusion

ML-3D BPM has been designed and fabricated to effectively store eight levels of magnetic information. We show the principles of recording and reading information from a ML-3D recording system via externally applied magnetic fields, the magneto-optical Kerr effect, and magnetic force microscopy. The MFM measurements clearly show the discretization of the magnetic signals emanating from the ML-3D BPM. These signals are further proven to be repeatable and distinguishable throughout the analyzed patterns. Furthermore, we show that ferromagnetic interaction between adjacent magnetic layers can be significantly reduced by amalgamating Co/Pt with Co/Pd multilayers media.

Now that it was verified that Co/Pd based media could be used for data storage operations, it was now possible to use the information that was found in the two preceding sections to begin to fabricate media for logic operations. In the following sections three different types of magnetic logic systems will be described. The media for each of these three systems will be fabricated from Co/Pd multilayers.

* Some of the material in this chapter was reprinted with permission from N. Amos, et al., *PLoS One*, vol. 7, no. 7, p. e40134, Jan. 2012.

Section 2 - Logic

Introduction

Semiconductor devices used for logic applications have been aggressively scaled down over the last half century. Conventional silicon-based logic technologies are approaching physical size limitations due to the current leakage effect in relatively small structures [43]. Therefore, an alternate technology is vital to continue decreasing the physical size of logic devices. This section addresses this issue by proposing three novel technologies, which are based on nanomagnetic logic devices. Three different methods for implementing magnetic logic gates will be described. The first type of magnetic logic gate is a dual-layer patterned magnetic media that can be implemented on a hard disk drive. Each of the patterned islands acts as a logic gate, where each magnetic layer of the dual layer media is an input. The output signal is read by the reading element of the hard disk drive to determine logic operations. The second proposed magnetic logic gate is a three-layer patterned magnetic media that can be implemented in a number of different ways; it may either be assembled in a hard disk drive or implemented as a 3D nonvolatile logic device. Finally, the third magnetic logic technology to be described utilizes a quad layer, patterned, magnetic media to create a reconfigurable logic cell. The bottom layer acts as a switch that determines if the logic cell acts as an AND or an OR gate. The two middle layers act as the two inputs for the gate. Lastly, the top layer acts as the output and the magnetization state of the output layer will determine if the output is a “1” or a “0.”

In the following sections, a brief background of logic devices along with the three proposed methods for implementing magnetic logic gates will be discussed.

Overview of Computer Logic

Boolean algebra is a system of mathematics/logic that forms the basis of all logic computations in modern day computers. It is a form of symbolic logic that was first described by George Boole (1815-1864). Many changes have been made to this system since Boole's time, but at the core it is still the logic that he described. Boolean algebra works with functions that have inputs and outputs that can only take on two values, true and false, or in the case of computers the binary values '1' and '0' respectively. In computers, '1' and '0' both correspond to different voltage values within in a circuit. There are three important Boolean functions that are used in computers today: AND, OR, and NOT. Collections of these gates are considered "universal:" in that with these three logical functions/gates any type of Boolean function can be realized. The AND gate has two inputs and one output. The output of this gate is '1' if and only if both of the inputs are '1' as well; otherwise the output is '0.' The OR gate, like the AND gate, has two inputs and one output. The output of an OR gate is '1' if either of the inputs are '1' as well. So, the output is '0' only when both of the inputs are '0.' The final function is the NOT gate or inverter. The NOT gate only has one input and one output. This gate flips whatever the input is. If the input is '1' then the output is a '0' and vice versa [44]. The truth table and circuit diagram for each of these functions can be seen in Figure 1. In modern computers, everything is carried out by NAND and NOR gates. These gates are AND gates and OR gates with an inverter connected at the output.

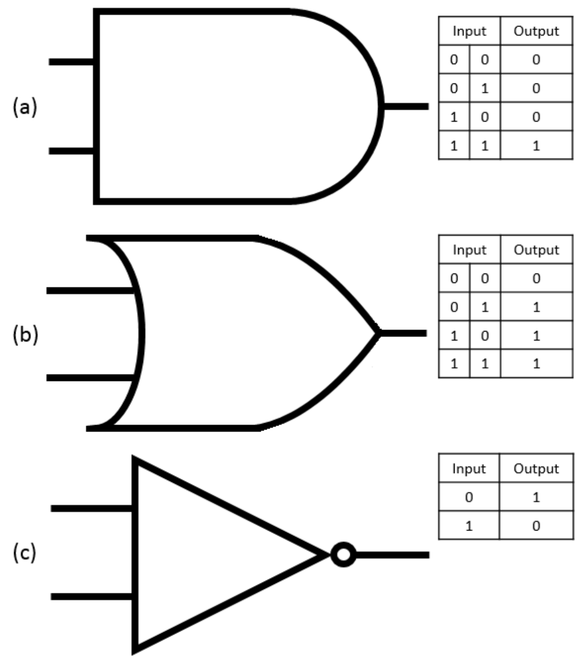

Figure 21: Circuit diagrams and truth tables for (a) AND Gate, (b) OR Gate, (c) NOT Gate.

Background

A number of different devices have been used to perform the operations of the three logic functions described in the previous section. First, electro-mechanical switches were used by the telephone company. These were replaced by vacuum tubes in the 1940s and ‘50s, and then replaced by transistors because they were error prone and bulky. After that individual transistors were wired together and now the operations are performed by billions of transistors fabricated on a single chip [44], [45]. Currently, there has been research into creating the logic gates using the principles of magnetics [46].

Transistors

The first semiconductor transistor was created at Bell Labs by Bardeen, Brattain, and Shockley in 1947 [47]–[49]. Improvement of the transistor eventually led to the fabrication of integrated circuits (ICs), which is a number of electronic circuits fabricated one substrate, usually silicon. In the 1970s, complementary metal oxide semiconductors (CMOS) ICs were invented. The CMOS technology is still prominently used today. At first there were a small number of transistors in a single IC, however today, there are billions of transistors in a single IC. This is because there was a rapid growth in the technology required to fabricate transistors at smaller and smaller scale as well as significant market forces encouraging the expanse of modern day computing power [50].

CMOS circuits have advantages over other type of transistors. One advantage is that they can be fabricated in a smaller area than BJT transistors. Another advantage is that both n-channel and p-channel devices can be fabricated on the same substrate. Therefore, their logic functions are carried out by circuits that contain both types of transistors. There are three basic principles of operation for CMOS transistors. The n-channel device conducts when the gate-to-source voltage is equal to zero. The p-channel conducts when the gate-to-source voltage is a negative value. The final principle is that either device will turn off when its gate-to-source voltage is zero [51].

Although transistors themselves are extremely small, it takes four transistors to make up NAND and NOR gates with current CMOS technologies [50]. Also, when semiconductor manufacturers mention the minimum feature size of their transistors, this is the size of one portion of one transistors. Although transistors are extremely small, to create one gate it still takes up a substantial amount of space. This will be one of the main disadvantages of current semiconductor technology when compared to magnetic logic gates. In the magnetic logic gates that will be described in the coming sections, each gate is contained in one single patterned island.

Magnetic Logic

The idea of magnetic logic devices is not new. In the 1950s-60s, research groups were already working on all-magnetic logic computing. At that time, their main advantage over transistors was that they were practically indestructible when compared to vacuum tubes. These devices were relatively large because they consisted of magnetic ferrite elements interconnected with copper wires. The logic state of the device was determined by the direction of magnetization, clockwise or counterclockwise. Due to the rapid advancements of integrated circuits, they were never able to keep up with transistor technologies [52], [53]. Around the same time, other research groups proposed all-magnetic logic using magnetic thin films. Their research focused on domain tips (DOT) logic devices. In these devices, the domain tips were propagated through low coercivity force channels that were fabricated in magnetic films with high coercivity. There were three important properties that were utilized to create these devices: (1) direction of domain tip propagation was dependent on the direction of the applied field, (2) the interactions between domain tips and (3) domain tip speed of propagation [54]–[56]. This research can be considered a precursor to the domain wall logic that is being explored today.

Recently, there has been a renewed interest in magnetic logic computing. Current developments include work on magnetic domain wall logic [23], combinations of magnetic and semiconductor logic [57], and magnetic quantum-dot cellular automata [58]–[60]. These technologies are mainly based on longitudinal magnetic thin films. Nonetheless, not all research has been focused on longitudinal media. Some recent research on nanomagnetic logic implemented perpendicular magnetic thin films. One group successfully created a 1-bit full adder using perpendicular multi-layered magnetic media. The group used a focused ion beam of gallium atoms to partially irradiate the media to locally adjust its anisotropy. This created a nucleation center that was used to propagate the signal through the magnetic logic device [61], [62]. Another group was able to fabricate stacked magnetic layers to generate a magnetic ratchet for logic applications [63]. They made use of antiferromagnetically coupled magnetic layers to shift a soliton from one layer to another. The three magnetic logic structures that will be described in the following sections will rely on both perpendicular media and exchanged-decoupled magnetic layers. This way each magnetic layer can be switched independently of the other layers and not be affected by the other layers in the stack. Furthermore, since we adopted perpendicular magnetic media, we are able to make a stacked gate that is relatively smaller than its longitudinal counterparts. Hence, gaining a crucial advantage over other similar technologies that use longitudinal media.

Multilevel Patterned Magnetic Media for HDD-based Nanomagnetic Logic

Introduction

Semiconductor devices used for logic applications have been aggressively scaled down over the past decades. In today's silicon based logic device technology, the physical gate length is approaching its physical limitations due to the need to decrease the device pitch in order to reduce the physical size of the memory cell [43]. Therefore, it's imminent that a new technology is needed in order to continue decreasing the physical size of logic devices. One possible technological solution for this problem is multilevel nanomagnetic logic implemented on a hard disk drive. This technological alternative presents a number of advantages for silicon based logic devices. The first potential advantage is that modern magnetic technologies are currently capable to create features of less than 10 nm in size [64]. This will allow for high integration density (2D & 3D) and is only limited by the size of the island or of the recording device [65]. Second, since the logic gates will be implemented on a hard disk, this will allow for high speed room temperature operation. The speed of operation is limited by the rotation of the disk, which is ~10 m/s. This speed allows for a feasible data rate of ~ 1 Gigabit/second for a single channel. Theoretically, these devices will have negligible power consumption when compared to semiconductor devices. With magnetic logic gates, the majority of the power consumption comes from the rotation of the disk, not from the gates themselves. Third, magnetic logic devices are an attractive option for harsh environment applications due to their inherent resistance to ionization radiation and electromagnetic shock waves, making the device especially attractive for military applications.

Concept

Safonov has recently proposed a method for performing magnetic logic operations on a hard disk drive, using two perpendicularly oriented grains [46]. What we plan to propose is similar in theory to this, but different in the implementation. While Safonov's proposal was to carry out logic using two perpendicularly oriented grains, our proposal is to carry out logic on a dual layer, patterned magnetic media. This is accomplished by creating a two layer perpendicular magnetic media that is capable of exhibiting three distinct levels of magnetization, as seen in Figure 22.

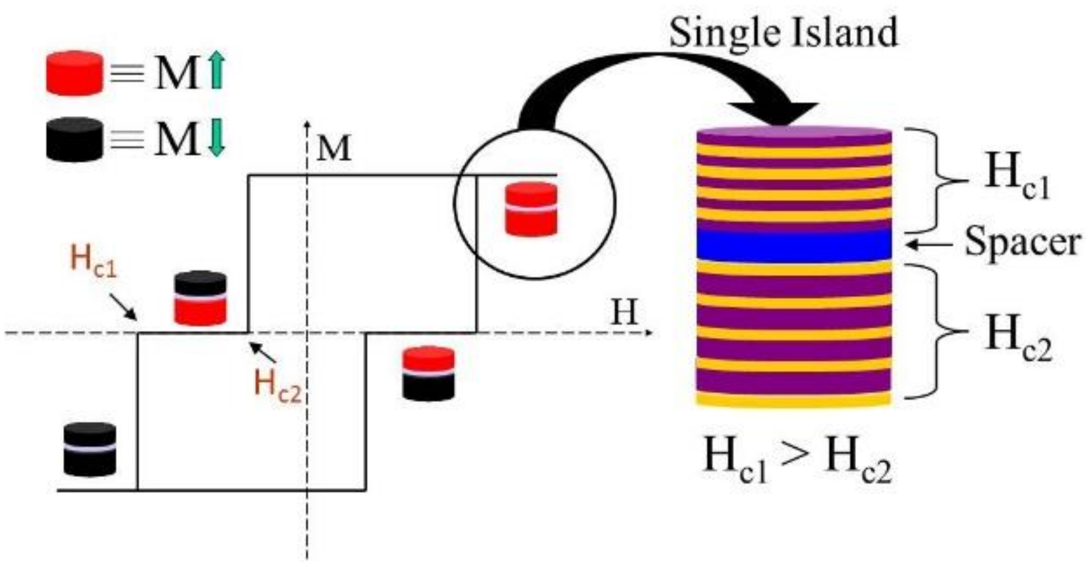

Figure 22: This shows the theoretical two layer media that exhibits 3 distinct levels of magnetization.

In order to record data in each layer individually, both layers must have different coercivity values. In this case the, the top layer has a greater coercivity value (HC1) than the bottom layer (HC2). Also, in order to have three distinct output states instead of four, the magnetic moment of each layer must be nearly the same. This will allow the magnetization of the stacked structure to be nearly zero when the magnetization of each layer is in opposite directions. To record data on the media, first a strong magnetic field ($|HREC| > HC1$) is applied to the media by the recording head. This will align the magnetization of both layers into the same direction. Next, the bottom layer's magnetization can be switched by the recording head by applying a recording field that is equal to the coercivity value of the layer ($|HREC| \approx HC2$). Once both of the layers have been magnetized, it is now necessary to read the signal and determine what type of logic was carried out. Each logic cell is made up of two magnetic domains side by side, as can be seen in Figure 23.

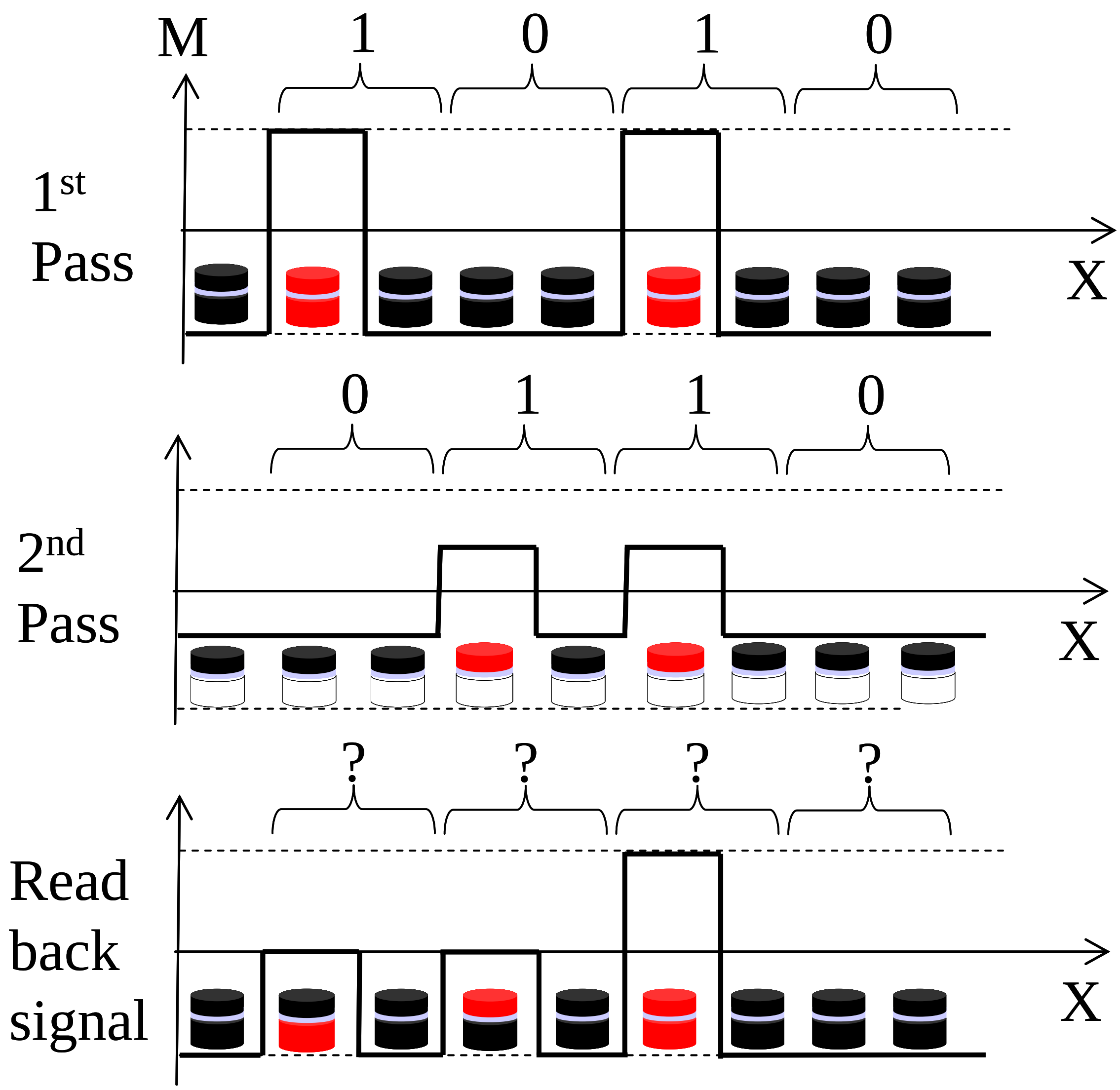

Figure 23: These graphs show the two clock pulses that are required to write the two input signals to the magnetic media. The third graph displays the output signal that is to read by the read head of the HDD.

One of the cells is always in the "↓↓" state, this will help with reading the output signal. Depending on the way that the output signal is read, the stacked structure can act as either an AND gate or an OR gate. If the output signal is read by a simple peak detector, the logic cell will act as an OR gate. In this case, each stack is compared to the domain in the "↓↓" state. If the output is any other signal is anything besides the "↓↓" state, it reads that as a "1." If the output state is read by an extra peak detector, the logic cell will act as an AND gate. Again, the output signal is compared to the signal of the domain next to it. In this case, the only output signal that is read as a "1" is when the output is in the "↑↑" state, otherwise the output is read as a zero. For these devices, the truth table can be seen in Table 1. For our media, a magnetic domain in the "↑" direction corresponds to a binary "1," while a magnetic domain in the "↓" direction corresponds to a binary "0."

IN1	IN2	OR	AND
0	0	0	0
0	1	1	0
1	0	1	0
1	1	1	1

Table 1: Truth Table for the logic gates.

Fabrication

In order to effectively stack decoupled magnetic layers (each exhibiting a unique coercivity value) across the bulk of the media, fabrication conditions and media compositions, which alter the coercivity field of Co/Pd multilayers, have been investigated as a prerequisite for the ML3D media integration. The coercivity field dependence on the substrate composition and processing pressure has been studied. These results were shown in previous sections. Following the coercivity dependence analysis, the following dual stack Co/Pd ML3D media with a composition of was chosen:

Pd(5 nm)/{Co(0.36 nm)Pd(0.55 nm)}x7/

Pd(5.3 nm)/{Co(0.36 nm)Pd(0.55 nm)}x7/Pd(5.3 nm)

This composition is sputter-deposited with a processing pressure of 5 mTorr and 30 mTorr for the first and second Co/Pd multilayers stacks, respectively. The out-of-plane and in-plane components of magnetization are then measured via polar magneto-optical Kerr microscopy (P-MOKE). Our results reveal that the processing pressure can be an effective parameter to alter the coercivity field of Co/Pd multilayers stacks and that a palladium interlayer above ~3 nm is sufficient to exchange-decouple the magnetic layers.

After the composition of the dual layer media was optimized, it was now time to fabricate the patterned media. For this application, we chose to deposit the media onto a pre-patterned SiO_2 on Si substrate. There are a number of lithographic steps that went into fabricating the prefabricated media. A schematic of the process can be seen in Figure 24. First, poly(methyl methacrylate) (PMMA) is spin coated onto the wafer. Next, the sample is placed in an e-beam lithography to write/expose the patterns into the resist. After the sample has been exposed, it is place in a developer to lift off the exposed areas. Then, we deposited Cr onto the sample via e-beam evaporation. This is then followed by liftoff of the remaining resist and reactive ion etching (RIE) of the Cr protected sample.

After RIE, the Cr was removed via wet etching. Finally the dual layer magnetic media was deposited via plasma enhanced ion sputtering. A more in-depth description of this process by Beomseop *et al.* [64]. After all of the steps mentioned above, it is now time to test the sample to determine if we are able to get the output signals that were described in the concept section.

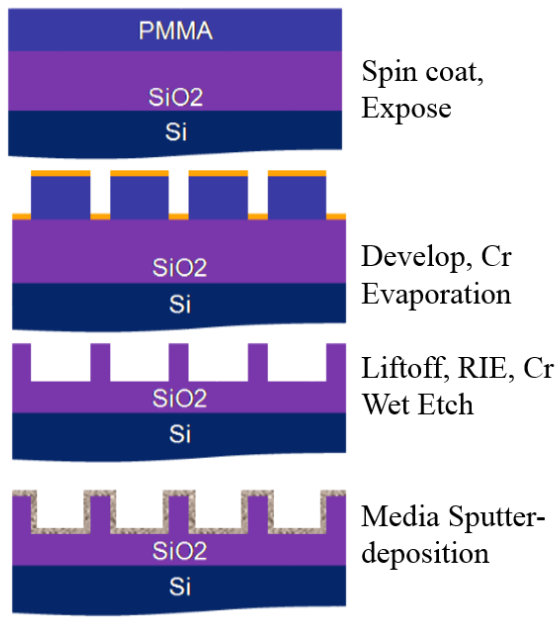

Figure 24: Schematics of the EBL Process for BPM.

Magnetic Force Microscopy (MFM) Study

In order to test the output signal of the pre-patterned magnetic media, we chose to perform a magnetic force microscopy (MFM) study of the sample. In order to properly test the magnetic media using MFM, we had to use a custom fabricated MFM probe. There were two important properties of the probe that we needed to take into account.

First, the probe needed to have a high enough magnetic moment in order to sense all three of the possible output states and it also needed to be low enough so that it would not switch the magnetic state of the logic cell that it was imaging. The second property that needed to be taken into account was the coercivity value of the probe. The probe needed to have a coercivity value that is higher than the field produced by the magnetic media, otherwise, it would be impossible to determine the output signal of the logic cell. Now that we had the MFM probe, there was one more step necessary before we could take the AFM/MFM image. It is necessary to randomize the magnetic states of the media, so that we are able to produce all 3 of the magnetic states in one image. To randomize the states of the media, the media was exposed to an alternating and decaying magnetic field. In Figure 25 (a)-(b), the resulting AFM and MFM images can be seen. This media is made up of logic cells of various diameters, ordered from larger diameters to smaller diameters from bottom to top. The AFM shows the size and shape of the logic cells. In the MFM image we are able to see the various output signals of each of the logic cells. As can be seen in the MFM image, the logic cells with larger diameters are not made up of a single domain. Therefore it is necessary to analyze the output signals coming from the smaller diameter logic cells. In Figure 25 (c), a cross sectional slice was taken to display all 3 of the possible magnetic states. The cross sectional signal was taken from the six logic cells that are boxed in red on the AFM/MFM images. In the cross sectional view, the black-dotted line corresponds to the AFM signal of that line and the blue-dashed line corresponds to the MFM signal of that line. The circled numbers in red mark each of the three possible states of the media. States 1 and 2 correspond to when both of the layers are magnetized in the same direction. The third state corresponds to when the two states are magnetized in opposite directions. Through the MFM study, we were able to prove the feasibility of the logic cells by displaying all three of the possible output signal magnetic states.

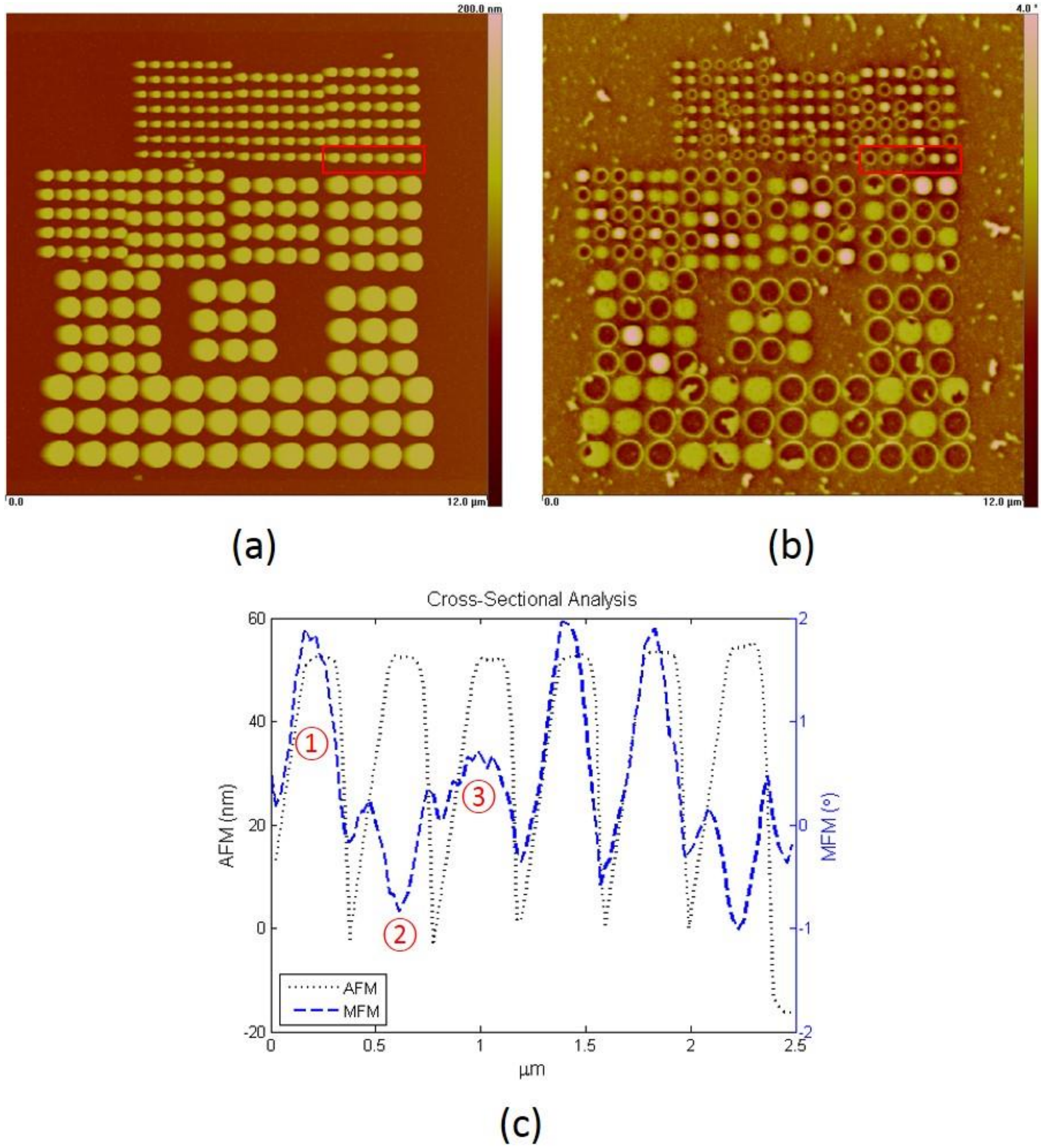

Figure 25: (a) AFM image of the patterned media, (b) MFM image of the patterned media, (c) Cross sectional view of the AFM (black) and MFM (blue) signals.

Conclusion

In conclusion, we described and tested a novel technology for creating nanomagnetic logic gates on a magnetic hard disk drive. We proposed a method to read and write signals to a dual layer patterned magnetic media. Next, we outlined the testing and fabrication process to create a media that exhibited the characteristics that were necessary in order to properly carry out our logic gates. Once we had the proper composition, it was then sputter deposited onto a pre-patterned substrate. Once we had a substrate with our logic gates on them, it was then time to test to make sure we were getting the three output signals that were described previously in the concept section. To verify the output signals, we did an MFM study of an array of logic gates of different sizes and then we focused in on a row of gates that exhibited all three of the possible output states. So, we set forth a concept on how these types of logic gates could operate and then we proved the feasibility of such gates by showing all of the possible output states with a MFM study of the sample.

Reconfigurable and Non-Volatile Vertical Magnetic Logic Gates

Introduction

Today, like never before, the electronics industry is looking for an alternative to semiconductor technology. This is because current semiconductor technologies are approaching fundamental limitations [43]. The most promising alternative to current technologies is magnetic logic devices or some hybrid of magnetic and semiconductor technology, which would take the best of the two technologies. There are a number of key advantages to using magnetic devices: fundamentally lower energy consumption, non-volatility, radiation hardness, ultra-high scalability and relatively high data rates [64], [65]. In this section, we present an experimental study on magnetic logic gates/cells that can be used to construct purely magnetic devices or be integrated with current semiconductor technologies.

Concept

Using Boolean algebra, it is possible to prove that any logic operation can be created with the three basic logic functions: NOT, AND, and OR [44]. It has been shown that the magnetic NOT gate can be created by two antiferromagnetically coupled cells being fabricated, therefore it will not be discussed [58]. The logic gates/cells that will be discussed in this section will consist of two inputs and a RESET. The purpose of the RESET is to determine if the gate will either be an AND gate or an OR gate. When the RESET is set to “0” the gate will work as an AND gate and when the RESET is set to “1” it will function as an OR Gate. The truth table for such gates can be seen in Table 2.

GATE	*STATE*	*RESET*	*Input 1*	*Input 2*	*Output*
AND	**1**	0	0	0	0
	2	0	0	1	0
	3	0	1	0	0
	4	0	1	1	1
OR	**5**	1	0	0	0
	6	1	0	1	1
	7	1	1	0	1
	8	1	1	1	1

Table 2: Truth table for the reconfigurable AND/OR gate.

In order to implement the logic gates that are discussed above, we designed a three-layer magnetic media to demonstrate the logic operations. There are at least a couple of possible ways that this media could be used; both ways have advantages and disadvantages. One possibility is to fabricate it as a homogeneous media, such as that used in conventional perpendicular magnetic recording disks [66]. The main advantage of this is the low fabrication cost. Existing magnetic recording media fabrication facilities can be used for this type of media. The other possibility is to use a patterned media to implement these gates. In this case, each logic gate would be physically separated from its neighboring cells. Thus, the possibility of magnetic fields from one device affecting the state of another device is minimized. Also, another advantage of this fabrication method is that the devices can be packed more densely together than in the continuous media, allowing for a greater number of devices per unit area. In order to create the patterned media, some type of lithography will be necessary, such as x-ray lithography, e-beam lithography, imprint lithography, or ion-beam lithography. In this section, our focus will be on the design and fabrication of the patterned media that can be used for such logic gates.

As described above, each of the magnetic layers will act as either an input layer or a RESET layer for the vertical logic gate. The logic operations will be carried out by the interactions between the magnetic fields that are created by each of the layers, as seen in Figure 26 (a)-(b). Each of the layers needs to be magnetically "hard" so that the field created by one layer does not affect the magnetization of the other two layers. In order to be able to selectively change each layer/input individually without altering the state of the others layers, each layer must have a unique coercivity. Hence, the media is designed with a gradient of coercivity values (H_C). The bottom layer ("Input 2") will have the lowest coercivity and the top layer ("Reset") will have the highest coercivity, such that: $H_{C\_input2} < H_{C\_input1} < H_{C\_reset}$. The "Reset" layer must have the highest value of coercivity so that its magnetization direction will not be changed when an input field is applied to the gate. The other important property of each layer is its magnetic moment. In order to distinguish the magnetic state of each layer during the readback process, the magnetic media must be fabricated in such a way that: $m_{input2} > 2m_{input1} > 4m_{reset}$, where *m* is the total magnetic moment of each layer.

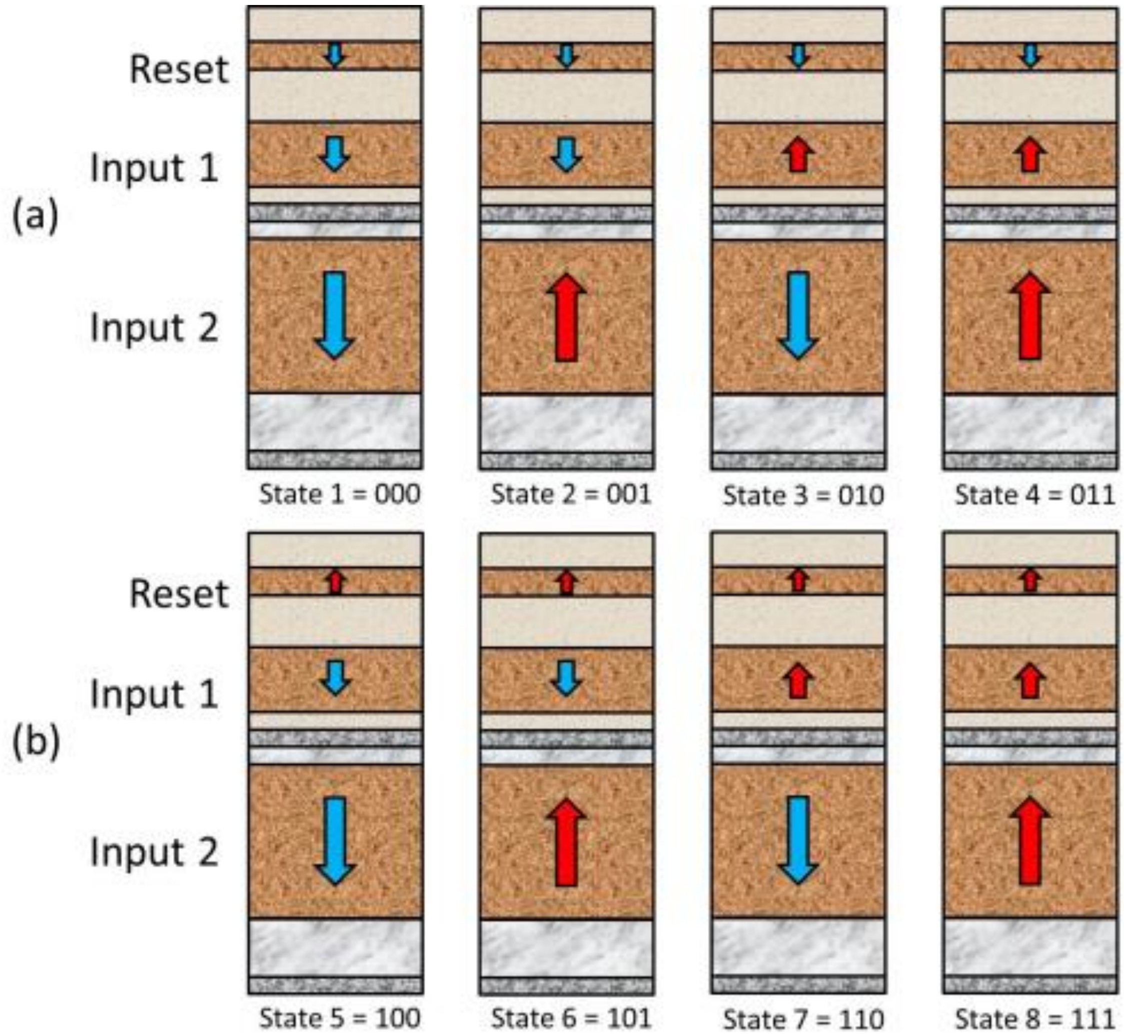

Figure 26: (a) AND, (b) OR gates of the three-layer reconfigurable magnetic logic gate. The direction of the magnetization determines if the bits is a 1 or a 0. "Up" = 1 and "Down" = 0.

Each of the magnetic layers will be designed to have perpendicular anisotropy, so they can be analogous to transistors. When the magnetization of the layer is in the "Up" direction, this will correspond to a binary "1" and when the magnetization is in the

“Down” direction, this will correspond to a binary “0.” The magnetization direction of the top RESET layer will determine if the stack will act as either an AND gate (Figure 26(a)) or an OR gate (Figure 26(b)), “0” and “1” respectively. For this study, the stacks will be fabricated to be square stacks that are 120 nm on a side and separated by 225 nm.

The main focus of this study is the theory and fabrication of 3D magnetic logic gate, but we will briefly describe methods for reading and writing to the inputs and reset layer. As will be shown in Sec. 0, the output of the logic gate can be read with an MFM probe. Another method would be to utilize the read/write heads of a hard disk drive to polarize each layer in a certain direction and then read the net magnetization of the stack to determine the output of the logic operation. In addition, a patterned array of nanomagnets or magnetic quantum-dot cellular automata can also be implemented to transfer inputs and outputs between the gates [67]. The latter method would be the most useful, because it would allow our magnetic logic gates to be integrated into existing semiconductor technologies. The inputs of the gates will be set by the effect of spin-torque transfer, in which a spin-polarized current is applied to set the direction of magnetization for each layer [68]. The output can be read using giant/tunneling magneto-resistive (TMR/GMR) sensors. The resistance of the output will change depending on the net magnetization of the 3 magnetic layers of the stack [69]. The effects of MTJ have been extensively studied by a number of different groups [70]–[75]. Recently, there has been a study, by Tanaka *et al.*, into the possibility of using microwaves to selectively switch the magnetization in a three-layered stacked magnetic structure.[76] Through micromagnetic simulations, they were able to show that it is possible to individually switch the polarization of each layer.

Although this research was conducted for uses in magnetic recording, it can be utilized to selectively switch each of the layers in our logic gates. These are just a few feasible methods that can be exploited to read and write information to the input and RESET layers.

Fabrication

Many different compositions were tested in order to optimize the media for this particular application. Following this evaluation, we optimized a composition that provided the necessary magnetic properties for the logic gates to function properly. Co/Pt and Co/Pd multilayers were chosen for the magnetic layers. This is because it is possible to fine tune the values of coercivity and magnetic moment of these materials. It has been shown that these properties can be controlled by the deposition parameters, thickness of each layer, and the number of bi-layers that make up each magnetic layer [42]. The following is the selected composition:

Substrate/Ti(1.5nm)/Pt(5nm)/[Co(0.4nm)/Pt(0.55nm)]x14/Pt(1.5nm)/Ti(1.5nm)/Pd(1.5nm)/[Co(0.25nm/Pd(0.55nm)]x7/Pd(4.5nm)/[Co(0.25nm)/Pd(0.55nm)]x3/Pd(3nm)/Ti(4nm)

A number of processes were used to fabricate the media for this experiment: (1) the magnetic media was sputter deposited onto a Si substrate, (2) Hydrogen silsesquioxane (HSQ) was spin coated and then baked onto the top of the media, (3) E-Beam lithography to generate the patterns onto the HSQ, (4) development of the patterns, (5) ICP etching of the oxidized Ti layer, (6) Ar-Ion milling of the media to transfer the patterns into the continuous media. A SEM image of the 120 nm diameter patterns can be seen in Figure 27. A more in-depth description of each of these processes is published elsewhere [77]. For this work, the coercivity of each patterned magnetic layer was estimated through MFM analysis. This is done by applying a range of magnetic fields to the media and then testing it after each exposure with MFM. Using this method, we were able to determine that the “Input 2” layer has a coercivity value 2.5 kOe, the “Input 1” layer is ~ 5.0 kOe, and the “Reset” layer is ~ 6.0 kOe.

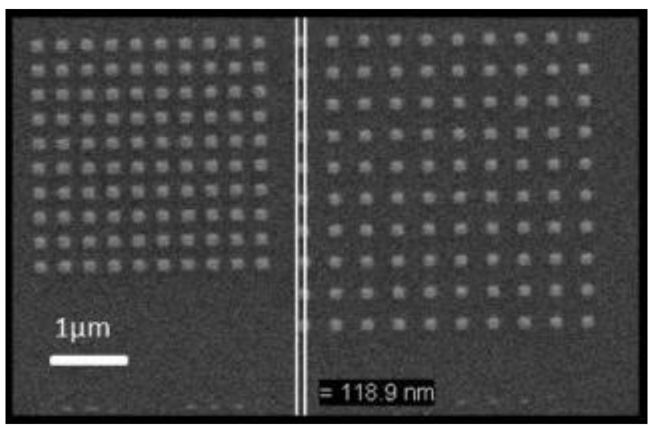

Figure 27: A SEM image of 120 nm diameter patterns.

Magnetic Force Microscopy (MFM) Study

Since the focus of this section is only the logic gate itself and not the input/output channels we will analyze the gates using magnetic force microscopy (MFM) imaging. Although, this is not how the gates will work in a device, the MFM study will give us insight on how the gates will perform once they are implemented at the device-level. The two properties that need to be taken into account for the MFM probe are the magnetic field strength and coercivity of the magnetic tip. The magnetic field strength of the tip should be high enough to differentiate the signals from the 3-layers logic cell, but not too high to switch their magnetization. The magnetic tip coercivity should be high enough such that the magnetic field emanating from the nanomagnetic cells would not switch the magnetization of the probe and cause difficulties in data interpretation. For this study, we used a *PSENS^{TM}MFM-UHC* probe with tip coercivity of ~ 1 Tesla. The probe was magnetized by the manufacturer with ~ 3 Tesla along the tip central axis. For all the images that were taken, the magnetization direction of the probe was out of the apex of the tip (Figure 28(a)). Both atomic force microscopy (AFM) (Figure 28(b)) and MFM images were taken of the media. To make the analysis easier, we will only focus on the pattern on the left, in the SEM image in Figure 27.

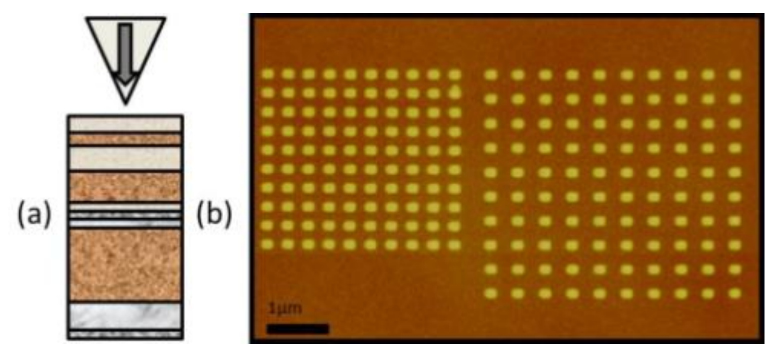

Figure 28: (a) Illustration of the direction of the magnetization of the probe with respect to the media, (b) An AFM image of the patterns that were used for the MFM study. The bits are 120 nm in diameter with different areal densities.

In order to view all eight of the possible states of this media with MFM, the two input layers needed to be randomized. To do this, the media was exposed to an oscillating and decaying magnetic field that started at 0.75 T and ended at 0.3 T. In order for the media to manifest the 8 possible input/reset combinations, the “Input 2” layer was polarized in the “Up” or “1” direction by exposing the media to a field of 0.3 T in the out-of-plane direction. The resulting MFM image can be seen in Figure 29(b). In Figure 29(c), each of the four possible states are highlighted in a different color and numbered so they can easily be differentiated from each other.

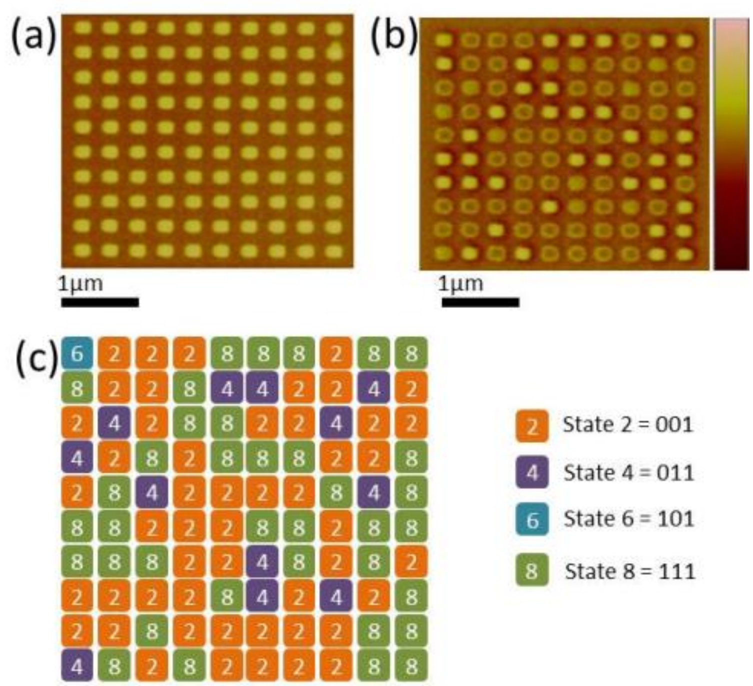

Figure 29: (a) AFM image, (b) MFM image of the 4 of the 8 possible input combinations, (c) An image created to highlight each of the individual four combinations with a different color and number, so that each one is easily distinguishable.

Next, the “Input 2” layer was magnetized in the “Down” or “0” direction by exposing the media to a field of ~ 0.3 T into the plane of the media. The resulting MFM image can be seen in Figure 30(b). As before, in Figure 30(c), a color coded and numbered image of the each of the 4 input combinations can be seen. Both images were taken in the same location, over 120 nm diameter patterns, with the same probe, with the height and phase scales the same. From these results, we can see that it is possible to fabricate a reconfigurable logic gate that has two inputs and one RESET, which allows the gate to work as an AND gate or an OR gate. From these two images we are able to observe all 8 of the possible magnetic states from this media. We were able to verify that states 3 and 6 were distinct states by cross sectional analysis. The reason there is only one instance of each state is attributed to the complexity of achieving such states with our method of magnetizing the sample.

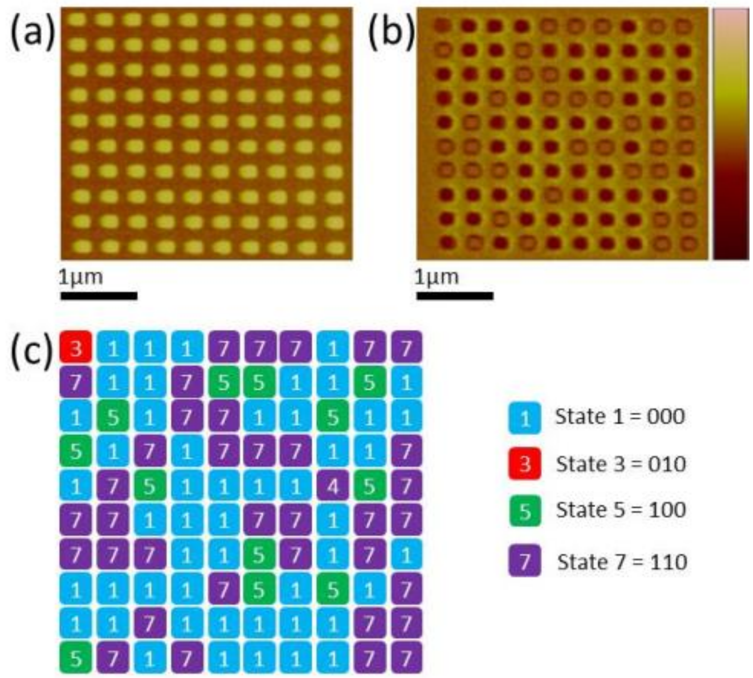

Figure 30: (a) AFM image, (b) MFM image of the other 4 possible input/reset combinations, (c) An image created to highlight each of the individual four combinations with a different color and number, so that each one is easily distinguishable.

Conclusion

In conclusion, we were able to fabricate and test a vertical magnetic logic gate that can be reconfigured to act as either an AND or and OR gate. The output of these gates depends on the states of the two input layers and the one RESET layer. In order to build the gates with a gradient of coercivity values and magnetization, Co/Pd and Co/Pt multilayers were used. By varying the thickness and number of Co/Pd and Co/Pt pairs in each layer, we were able to precisely control the coercivity values and magnetic moment.

We then used magnetic force microscopy (MFM) to analyze the logic operations of the patterned media and to determine that all 8 magnetic states were observable in this media.

* Some of the material presented in this chapter was reprinted with permission from J. Butler, et al. *J. Appl. Phys.*, vol. 115, no. 16, p. 163903, Apr. 2014. Copyright 2014, AIP Publishing LLC.

Three-dimensional Non-Volatile Magnetic Universal Logic Gates

Introduction

Modern magnetic technologies have potential for device scalability down to a nanometer logic bit or cell size [65]. The key potential advantages of magnetic devices include: (1) extremely low power consumption and negligible heat dissipation, (2) non-volatility, (3) radiation hardness, and (4) inherent extendibility into a dynasty of three-dimensional and multilevel technologies. In this section we present an experimental study of a magnetic logic gate that could be extended into a future class of three-dimensional (3D) fully integrated magnetic computer chips.

Any basic computing circuit consists of three major parts including: (1) input and output, (2) data channels, and (3) logic cells/elements/gates, respectively [58]. The input and output are tailored to a particular application. For instance, for the purpose of integrating magnetic circuits with existing semiconductor transistor chip technologies, the input mechanism can be provided through the effect of spin momentum transfer, in which a spin-polarized electric current through tunneling junctions is used to magnetize the input cells [68]. The output mechanism can be provided through a giant magneto-resistive effect in tunneling junctions, in which the resistance of output cells changes depending on the directions of the magnetization in the output cells [69]. The aforementioned effects in tunneling junctions as well as the physics of magnetic channels have been extensively studied by different groups [70]–[72]. In the current study, we focused on the third component of the circuit, i.e., the logic cells that can be built into a 3-D form and potentially represent a single universal gate, the basic element for reconfigurable magnetic computing.

3-D Logic Devices

A. 3-D Device Architecture

According to Boolean algebra, any logic operation can be built from three basic functions, AND, OR, and NOT, respectively [44]. The inverting magnetic NOT gate can be trivially implemented with two antiferromagnetically coupled cells, as shown in Figure 31(a), and therefore is not discussed [58]. The focus of this section is on a study of a four-layer 3-D magnetic cell structure which could be reconfigured as an OR or an AND gate. Schematics of AND and OR modes in the four-layer implementation of a reconfigurable AND/OR gate are shown in Figure 31(b) and Figure 31(c), respectively. Before we go into details, it can be mentioned that in the current 3-D configuration both continuous, i.e., non-patterned, and patterned 3-D structures could be used to accomplish the logic functions. The continuous structure would be similar to the continuous magnetic medium as it is used in conventional magnetic recording [66]. The key advantage in this case is the relatively cost-effective fabrication process. The magnetic "cells" could be defined by the gradient of the recording magnetic field which could be generated either by one moving transducer, as in conventional recording, or by a periodic 2-D set of stationary transducers placed on top of the recording media [21]. On the contrary, in the patterned structure, the logic cells are physically (not just magnetically) separated from each other and therefore some sort of patterning, e.g., UV-photo-, electron-beam-, imprint-, or another lithography technique, must be employed. In this case, the natural advantage of the higher packing density would come at the hefty cost of fabrication. Nevertheless, in this study we focused on a patterned media because it was well known that the latter had advantages with respect to thermal stability and consequently scaling to higher area densities [78].

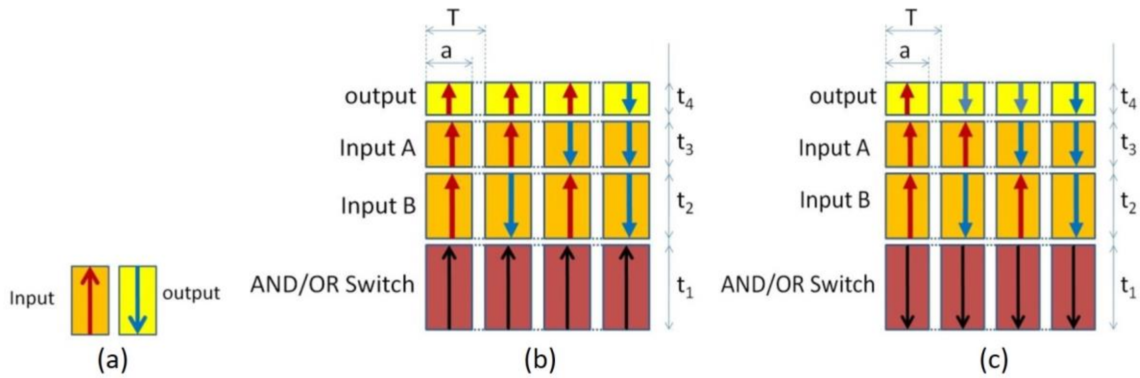

Figure 31: (a) Two antiferromagnetically coupled adjacent cells to represent an inverter, NOT gate, (b) AND, (c) OR modes of a four-layer reconfigurable gate implementation. "Up" and "down" magnetization directions denote bits "1" and "0" respectively (↑= “1”, ↓= “0”).

The media parameters were optimized with help of public-domain micromagnetic simulation package OOMMF, which was developed at National Institute of Standards and Technology (NIST) [79]. We used perpendicularly oriented magnetic media with the magnetization in “upward” and “downward” directions to define information bits “1” and “0”, respectively. Particularly, as natural 3-D building blocks, we exploited exchange coupled Co/Pd multilayers, which due to their relatively high perpendicular magnetic anisotropy had been used in conventional perpendicular magnetic recording [80]. One of the advantages of the multilayer structures especially important for the discussed 3-D applications is the fact that their properties, such as the coercivity and the saturation magnetization, could be significantly varied within the thickness of the film through the control of deposition conditions, as described below. In turn, the presence of the property gradients within the thickness allowed access to different layers during write/read processes and thus helped accomplish the targeted 3-D operation. Furthermore, in the future Co/Pd multilayers could be mixed with Co/Pt multilayers to provide an even wider range of properties within the thickness of the 3-D media. However, for the sake of simplicity of the concept demonstration this study was limited to Co/Pd multilayers.

B. How 3-D Logic Devices Work

According to the discussed 3-D device architecture, each layer of the 3-D magnetic media represented a logic input or output, while the magnetic interaction between input and output layers fulfilled a logic function of interest. As illustrated in Figure 31(b)–(c), the particular device consisted of three "hard" input layers with different coercivity values, further referred to as RESET and two INPUT layers, respectively, and one "soft" output layer. Again, the physics underlying the operation of the logic device was the fact that the magnetic state of the output layer depended on the magnetic states of the three input layers. Using AND mode as an example, below we explain how logic functions could be performed with the 4-layer 3-D device. To switch the gate into this mode, it was necessary to magnetize the highest coercivity bottom layer in the downward direction, as illustrated in Figure 31(b). Because of the highest coercivity, this layer, referred to as RESET layer in this particular study, served as the MAJORITY gate according to a more widely accepted definition. Depending on the orientation of the magnetization in this layer, the system operated as either an AND or an OR gate. In this particular example, the “downward” and “upward” orientations triggered AND and OR gates, respectively. The net magnetic field within the layer, which is the sum of the demagnetization field and the field generated by the magnetic moments in the other layers (independent of their magnetic states), always remained smaller than its coercivity value of approximately 3.36 kOe. Therefore, the RESET layer indeed maintained its programmed magnetic state until it was intentionally switched (reprogrammed) to the other function mode, i.e., OR. Similarly, the coercivity values of the two INPUT layers were engineered to be over 2 kOe and over 1 kOe, respectively, and also could be considered as relatively “hard” layers in the particular field environment (with the maximum stray field of less than 0.7 kOe). The information between the input and outputs of these types of reconfigurable gates could be transmitted using a well-studied patterned array of nanomagnets (nanocells or cells) also widely known as magnetic quantum-dot cellular automata (MQCA) [67]. The magnetic properties of the cells are chosen so that their magnetic states are bi-stable to reflect the binary nature of computing. In other words, similarly to the current implementation, one of the two possible magnetization directions is selected to be the binary “1” or “0,” respectively. By building a network of nanocells, all functions of signal transmission can be realized through the magnetic coupling effects [81]. Interestingly, data channels built of such networks of nanocells could also be built in a 3-D form using the same multilayer material platform (as in this particular study). A study of the 3-D channel implementation using Co/Pd multilayers was presented at the recent

55th Magnetism and Magnetic Materials (MMM) Conference in Atlanta, Georgia [24]. Going back to this study (of logic gates), the estimates were made for a square periodic pattern with a pitch of 80 nm and a square cell with a side of 50 nm, corresponding to a one-layer packing density of above 100 Gigacells/layer/in^2. In general, the difference in coercivity between the two INPUT layers could be used to distinguish ("labeling") the inputs from each other during the write operation. However, it should be remembered that in certain cases it could be advantageous to maintain similar values to ensure physical equivalency of different inputs.

As the OUTPUT layer, the lowest coercivity layer, with H_c of below 0.15 kOe, was used. The output layer was the only "soft" layer in the stack in the sense that its remanent state was defined by the magnetic states in the other three layers. Again, the other three (hard) layers had substantially higher coercivity values ranging from somewhat less than 1 to over than 3 kOe to ensure that a local field in the system could never affect their magnetic states. On the contrary, the coercivity of the output layer was selected to be smaller than the net local field so that its magnetic state depended on the magnetic states of the (hard) input layers and therefore could be identified with logic operations under study. Depending on the magnetic state of the RESET layer, the field from either one of the INPUT layers alone or both INPUT layers together was necessary to switch the magnetization in the OUTPUT layer. Going back to Figure 31(b) and Figure 31(c), it can be seen that having the RESET layer in states "0" and "1" ensured the logic modes AND and OR, respectively. The truth table for the reconfigurable 4-layer 3-D AND/OR gate is shown in Table I.

Input A	1	1	0	0
Input B	1	0	1	0
Reset = 0 (AND) Output	1	0	0	0
Reset = 1 (OR) Output	1	1	1	0

Table 3: Truth table for a reconfigurable AND/OR gate. AND and OR modes are determined by Reset = 1 and 0, respectively. The logic functions are defined by a code format (Input A, Input B, Reset, Output) as states on the hysteresis curve measured via magneto-optical Kerr effect.

Besides creating the described coercivity gradient, another design goal was to create a non-zero magnetization gradient across the 3-D media thickness. The presence of non-zero magnetization gradient was important to ensure that all the input layers adequately contributed to the net field in the OUTPUT layer despite the fact that the input layers were not equivalently located with respect to the output layer. For instance, the RESET layer, at the farthest distance from the OUTPUT layer, was chosen to have the highest magnetic moment. On one hand, it was important to increase the magnetization in each layer to maximize the signal-to-noise ratio (SNR). On the other hand, to avoid any undesired "erasure" of information, we limited the magnetization in each of the three input (hard) layers to values for which the local demagnetization and other layers' field was below the local coercivity. This tradeoff was important in defining the magnetization values in different layers in the 3-D device.

Figure 32 illustrates the four-layer media structure designed according to the described guidelines. The targeted relationships between the magnetic moment and coercivity values in each of the four “multilayer” layers could be approximately evaluated through the following relations: $m_4 = 2m_3 = 4m_2 = 8m_1$ and $H_{c4} > H_{c3} > H_{c2} > H_{c1}$. In this case, the effective magnetization was roughly proportional to the number of pairs in each strongly coupled multilayer stack (“layer”). Thus optimized locally averaged values of the magnetization of the four “layers” were approximately equal to 425, 305, 180, and 115 emu/cc, respectively, while the coercivity values were engineered to 3.2, 2.4, 1.1, and 0.5 kOe, respectively.

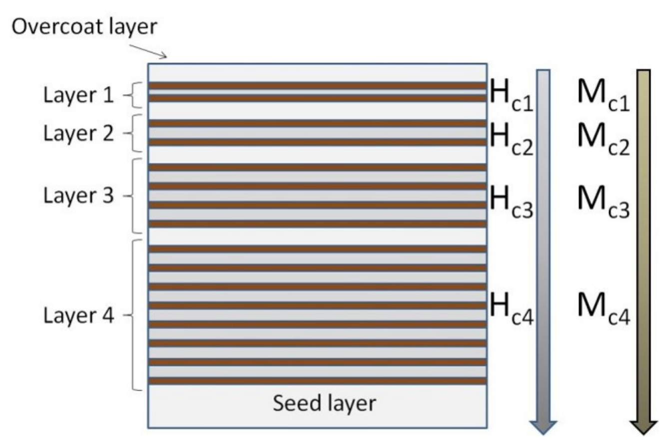

Figure 32: An illustration (not to scale) of the 4-layer 3D media configuration

C. Fabrication

Co/Pd multilayer films were deposited via co-sputtering on glass substrates in an AJA Orion 5 system. Prior to deposition, the glass substrates were Ar^+ milled using RF substrate biasing with a power of 25 W at a 5 mTorr pressure for approximately 2 minutes. A base pressure below 1×10^{-7} Torr was set for all samples. To improve thin film uniformity, the sample holder was rotated at approximately 40 RPM. The Pd seed/capping layers and the Co/Pd bilayers were deposited at a processing pressure of 5 mTorr and 15 mTorr, respectively. The Pd seed and capping layers were deposited at a rate of 0.43 Å/s while the Co and Pd layers were deposited at a rate of 0.35 and 0.63 Å/s, respectively. We exploited a combinatorial synthesis process to select optimized material compositions necessary to control gradients of the coercivity and the magnetization across the thickness, as described above [82]. To create the targeted gradients, we varied the relative thicknesses of Co and Pd layers in each pair and the number of pairs, respectively. For instance, films with two Co/Pd pairs in each, with four sets of Co and Pd thickness values, 0.45/0.85, 0.55/0.20, 0.55/0.25, 0.55/0.40 (nm/nm), respectively, provided coercivity values of approximately 0.15, 1.1, 2.4, and 3.2 kOe, respectively. The exact composition of the four-layer 3-D structure tailored to the model described below was the following:

Substrate/

Pd(5 nm)/Pd(0.7 nm)/{Co(0.4 nm)/Pd(0.7 nm)}×8/

Pd(5 nm)/Pd(0.7 nm)/{Co(0.4 nm)/Pd(0.7 nm)}×4/

Pd(5 nm)/Pd(0.7 nm)/{Co(0.4 nm)/Pd(0.7 nm)}×2/

Pd(5 nm)/Pd(0.7 nm)/{Co(0.2 nm)/Pd(0.7 nm)}×2/

Pd(5 nm)

D. Focused Magneto-Optical Kerr Measurements

The M–H hysteresis loop for the entire logic stack is shown in Figure 33, where the color lines show minor loops characterizing different possible magnetic states. The loop was measured using the polar signal in a Focused Magneto-Optical Kerr Effect (F-MOKE) system with a focusing length of less than 1 micron. The major and minor loops shown in Figure 33 demonstrate that it is possible to get all sixteen of the possible states from the media composition described in the previous section.

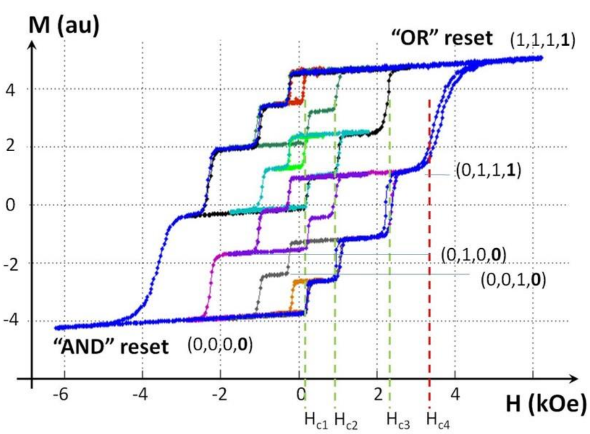

Figure 33: A Kerr-effect measured full M-H hysteresis loop. Minor loops are shown by different colors. The magnetic states in the four layers corresponding to different shoulders of the loop are coded as: AND/OR reset, IN B, IN A, and Output.

Conclusions

In conclusion, we presented an experimental study of a 3-D nanomagnetic 4-layer structure with a net thickness of less than 30 nm to enable a logic cell with reconfigurable AND and OR functions. The magnetic state of the "soft" layer, interpreted as the

OUTPUT layer, depended on the magnetic states of the remaining three “hard” layers, interpreted as two INPUT layers and one RESET layer, respectively. One of the advantages of using a 3rd spatial dimension was scalability of logic cells to ultra-high densities due to the ability to deposit active layers on top of each other. To build vertically oriented magnetic devices with a gradient of the coercivity and the magnetization across the thickness, Co/Pd multilayers were used. A combinatorial synthesis technique was exploited to vary the coercivity and saturation magnetization values accordingly through controlling the number of Co/Pd pairs and thicknesses of Co and Pd layers in each pair. We conducted focused magneto-optical Kerr effect (F-MOKE) measurements to understand the magnetization switching during logic operations. The next step to further this research would be to fabricate a patterned media similar to that used for the magnetic logic gates that were made up of three multilayers. Once the patterned media is fabricated, it would then be possible to test the gates using an AFM/MFM system. Results from an AFM/MFM study would demonstrate the feasibility of a logic gate fabricated from this composition.

*Some of the material in this chapter was reprinted with permission from N. Amos, et al., *J. Nanoelectron. Optoelectron.*, vol. 6, no. 2, pp. 132–137, Jun. 2011.

Section 3 - Conclusion

In conclusion, throughout this dissertation a number of novel technologies have been described that would be able to help overcome the fundamental limits that are being reached in current semiconductor and data storage technologies. In each section, the proposed research was designed, fabricated, and tested to prove the feasibility of implementing these technologies into the real world. First a study of Co/Pd multilayers as a candidate material for next generation data storage technologies showed that it was possible to specifically tailor the properties of the multilayers to whatever is needed for the particular application whether it be data storage or logic. Then, a three layer patterned magnetic media made up of Co/Pd and Co/Pt multilayers was designed and fabricated and then tested using magnetic force microscopy to prove the feasibility of store data in three dimensions. Following that, three novel approaches to magnetic logic gates were reported on. First, a dual layer patterned magnetic media made up of two Co/Pd multilayers was proposed to implement magnetic logic gates on a hard disk drive. The theory of operation, design, fabrication, and MFM study were presented. Second, a three layer patterned magnetic media was proposed to implement reconfigurable magnetic logic gates. These logic gates could be implemented on a HDD or combined with magnetic quantum-dot cellular automata to create a magnetic/semiconductor hybrid device. The theory, design, and fabrication of these logic gates were proposed and then a MFM study was carried out to prove the feasibility of the gates. Third, a four layer magnetic media made up of four stacked Co/PD multilayers was also proposed to implement reconfigurable magnetic logic gates. In these gates, the fourth layer would be used as an output layer. The design and fabrication of a quad layer thin film was proposed and focused magneto-optical Kerr effect measurements were carried out to determine that all sixteen of the possible states of thin film were achieved. The next step would be to fabricate a patterned media using the same thin film specifications and testing the feasibility of the logic with a MFM study.

Section 4 - References

[1] D. Weller and M. F. Doerner, "Extremely high-density longitudinal magnetic recording media," *Annu. Rev. Mater. Sci.*, vol. 30, pp. 611–644, 2000.

[2] G. A. Bertero, S. Malhotra, B. Bian, J. Tsoi, M. Avenell, D. Wachenschwanz, and T. Yamashita, "Longitudinal Magnetic Media Designs for 60–200 Gb/in^2 Recording," *IEEE Trans. Magn.*, vol. 39, no. 2, pp. 651–656, 2003.

[3] H. J. Richter, R. M. Brockie, and J. L. Pressesky, "Linear Density Dependence of Thermal Decay in Longitudinal Recording," *IEEE Trans. Magn.*, vol. 38, no. 1, pp. 260–270, 2002.

[4] S. N. Piramanayagam, "Perpendicular recording media for hard disk drives," *J. Appl. Phys.*, vol. 102, no. 1, p. 011301, 2007.

[5] W. a. Challener, C. Peng, A. V. Itagi, D. Karns, W. Peng, Y. Peng, X. Yang, X. Zhu, N. J. Gokemeijer, Y.-T. Hsia, G. Ju, R. E. Rottmayer, M. a. Seigler, and E. C. Gage, "Heat-assisted magnetic recording by a near-field transducer with efficient optical energy transfer," *Nat. Photonics*, vol. 3, no. 4, pp. 220–224, Mar. 2009.

[6] M. A. Seigler, W. A. Challener, E. Gage, N. Gokemeijer, G. Ju, B. Lu, K. Pelhos, C. Peng, R. E. Rottmayer, X. Yang, H. Zhou, and T. Rausch, "Integrated Heat Assisted Magnetic Recording Head : Design and Recording Demonstration," *IEEE Trans. Magn.*, vol. 44, no. 1, pp. 119–124, 2008.

[7] N. J. Gokemeijer, H. Zhou, D. Karns, S. Batra, M. Mallary, T. McDaniel, M. Seigler, G. Ju, Y. Peng, M. Xiao, and E. Gage, "Effect of gradient alignment in heat assisted magnetic recording," *J. Appl. Phys.*, vol. 105, no. 7, p. 07B905, 2009.

[8] L. Zhang, Y. K. K. Takahashi, A. Perumal, and K. Hono, "L10-ordered high coercivity (FePt)Ag–C granular thin films for perpendicular recording," *J. Magn. Magn. Mater.*, vol. 322, no. 18, pp. 2658–2664, Sep. 2010.

[9] M. K. Grobis, O. Hellwig, T. Hauet, E. Dobisz, and T. R. Albrecht, "High-Density Bit Patterned Media: Magnetic Design and Recording Performance," *IEEE Trans. Magn.*, vol. 47, no. 1, pp. 6–10, 2011.

[10] B. D. Terris, "Fabrication challenges for patterned recording media," *J. Magn. Magn. Mater.*, vol. 321, no. 6, pp. 512–517, Mar. 2009.

[11] Z. Yuan and B. Liu, "Double layer magnetic data storage - an approach towards 3D magnetic recording," *J. Magn. Magn. Mater.*, vol. 235, no. 1–3, pp. 481–486, 2001.

[12] S. Khizroev, Y. Hijazi, N. Amos, R. Chomko, and D. Litvinov, “Physics considerations in the design of three-dimensional and multilevel magnetic recording,” *J. Appl. Phys.*, vol. 100, no. 6, p. 063907, 2006.

[13] P. F. Carcia, A. D. Meinhaldt, and A. Suna, “Perpendicular magnetic anisotropy in Pd/Co thin film layered structures,” *Appl. Phys. Lett.*, vol. 47, no. 2, p. 178, 1985.

[14] F. J. A. den Broeder, H. C. Donkersloot, H. J. G. Draaisma, and W. J. M. de Jonge, “Magnetic properties and structure of Pd/Co and Pd/Fe multilayers,” *J. Appl. Phys.*, vol. 61, no. 8, p. 4317, 1987.

[15] B. M. Lairson, J. Perez, and C. Baldwin, “Pd/Co multilayers for perpendicular magnetic recording,” *IEEE Trans. Magn.*, vol. 30, no. 6, pp. 4014–4016, 1994.

[16] Y. Kubota, D. Weller, M. Wu, X. Wu, G. Ju, D. Karns, and J. Yu, “Development of CoX / Pd multilayer perpendicular magnetic recording media with granular seed layers,” *J. Magn. Magn. Mater.*, vol. 242–245, no. 1, pp. 297–303, 2002.

[17] S. Matsunuma, A. Yano, T. Koda, T. Onuma, H. Yamanaka, and E. Fujita, “Cross-sectional control of boron contents and the microstructures of Co/Pd multilayer perpendicular magnetic recording media,” *IEEE Trans. Magn.*, vol. 40, no. 4, pp. 2492–2494, 2004.

[18] W. W. Jiang, J. P. Wang, and T. C. Chong, “[CoAl/Pd] n multilayers as perpendicular recording media,” *J. Appl. Phys.*, vol. 91, no. 10, p. 8067, 2002.

[19] N. Speetzen, B. J. H. J. H. Stadler, E. Yuan, R. H. Victora, X. Qi, J. H. H. Judy, N. Supper, and T. Pohkil, “Co/Pd multilayers for perpendicular magnetic recording media,” *J. Magn. Magn. Mater.*, vol. 287, pp. 181–187, Feb. 2005.

[20] H. J. Richter, “Density limits imposed by the microstructure of magnetic recording media,” *J. Magn. Magn. Mater.*, vol. 321, no. 6, pp. 467–476, Mar. 2009.

[21] S. Khizroev and D. Litvinov, “Perpendicular magnetic recording: Writing process,” *J. Appl. Phys.*, vol. 95, no. 9, p. 4521, 2004.

[22] G. A. Prinz, “Magnetoelectronics,” *Science*, vol. 282, no. 5394, pp. 1660–1663, Nov. 1998.

[23] D. A. Allwood, G. Xiong, C. C. Faulkner, D. Atkinson, D. Petit, and R. P. Cowburn, “Magnetic Domain-Wall Logic,” *Science*, vol. 309, no. 5741, pp. 1688–92, Sep. 2005.

[24] Y. Tian, N. Amos, B. Hu, D. Litvinov, and S. Khizroev, “Considerations in the Design of a Highly Scalable Magnetic Logic Channel,” in *Proceedings of the 55th Annual Magnetism and Magnetic Materials (MMM) Conference*, 2010.

[25] B. J. McMorran, A. C. Cochran, R. K. Dumas, K. Liu, P. Morrow, D. T. Pierce, and J. Unguris, “Measuring the effects of low energy ion milling on the magnetization of Co/Pd multilayers using scanning electron microscopy with polarization analysis,” *J. Appl. Phys.*, vol. 107, no. 9, p. 09D305, 2010.

[26] R. Sbiaa, C. Z. Hua, S. N. Piramanayagam, R. Law, K. O. Aung, and N. Thiyagarajah, “Effect of film texture on magnetization reversal and switching field in continuous and patterned (Co/Pd) multilayers,” *J. Appl. Phys.*, vol. 106, no. 2, p. 023906, 2009.

[27] W. R. Bennett, C. D. England, D. C. Person, and C. M. Falco, “Magnetic properties of Pd/Co multilayers,” *J. Appl. Phys.*, vol. 69, no. 8, p. 4384, 1991.

[28] A. S. H. Rozatian, C. H. Marrows, T. P. A. Hase, and B. K. Tanner, “The relationship between interface structure, conformality and perpendicular anisotropy in CoPd multilayers.,” *J. Phys. Condens. Matter*, vol. 17, no. 25, pp. 3759–70, Jun. 2005.

[29] H. Hu, J. Pei, D. Xu, G. Qi, H. Hu, F. Zhang, and X. Liu, “Multi-level optical storage in photochromic diarylethene optical disc,” *Opt. Mater. (Amst).*, vol. 28, no. 8–9, pp. 904–908, Jun. 2006.

[30] S. Cui, S. Pu, G. Liu, and W. Liu, “Synthesis a New Photochromic Diarylethene for Electrochemical Switching and Holographic Optical Recording,” in *2009 Pacific-Asia Conference on Circuits, Communications and Systems*, 2009, pp. 536–539.

[31] A. Manfred, O. Hellwig, G. Hu, and B. D. Terris, “Method for magnetic recording on patterned multilevel perpendicular media using thermal assistance and fixed write current,” US 6865044 B1, 2005.

[32] A. Y. Dobin, H. J. Richter, and E. Girt, “Single-Pass Recording of Multilevel Patterned Media,” US 20100020437 A1, 2010.

[33] M. F. E. Erden, M. Benakli, and W. R. Eppler, “Multi-level recording on shingled coherent magnetic media,” US 7982994 B1, 2011.

[34] P. Shah, M. Ahmed, M. Ambroze, C. Tjhai, and P. J. Davey, “Novel Soft-Feedback Equalization Method for Multilevel Magnetic Recording,” *IEEE Trans. Magn.*, vol. 43, no. 6, pp. 2280–2282, Jun. 2007.

[35] V. Baltz, S. Landis, B. Rodmacq, and B. Dieny, “Multilevel magnetic media in continuous and patterned films with out-of-plane magnetization,” *J. Magn. Magn. Mater.*, vol. 290–291, pp. 1286–1289, Apr. 2005.

[36] M. Albrecht, G. Hu, A. Moser, O. Hellwig, and B. D. Terris, “Magnetic dot arrays with multiple storage layers,” *J. Appl. Phys.*, vol. 97, no. 10, p. 103910, 2005.

[37] V. Baltz, A. Bollero, B. Rodmacq, B. Dieny, J.-P. Jamet, and J. Ferre, “Multilevel magnetic nanodot arrays with out of plane anisotropy: the role of intra-dot magnetostatic coupling,” *Eur. Phys. J. Appl. Phys.*, vol. 39, no. 1, pp. 33–38, 2007.

[38] P.-O. Jubert, A. Vanhaverbeke, A. Bischof, and R. Allenspach, “Recording at Large Write Currents on Obliquely Evaporated Medium and Application to a Multilevel Recording Scheme,” *IEEE Trans. Magn.*, vol. 46, no. 12, pp. 4059–4065, 2010.

[39] G. Winkler, D. Suess, J. Lee, J. Fidler, M. A. Bashir, J. Dean, A. Goncharov, G. Hrkac, S. Bance, and T. Schrefl, “Microwave-assisted three-dimensional multilayer magnetic recording,” *Appl. Phys. Lett.*, vol. 94, no. 23, p. 232501, 2009.

[40] S. Li, B. Livshitz, H. N. Bertram, E. E. Fullerton, and V. Lomakin, “Microwave-assisted magnetization reversal and multilevel recording in composite media,” *J. Appl. Phys.*, vol. 105, no. 7, p. 07B909, 2009.

[41] T. Koda, H. Awano, H. Hieda, K. Naito, A. Kikitsu, T. Matsumoto, K. Nakamura, and T. Nishida, “Study of high magnetic anisotropy Co⁄Pd multilayers for patterned media,” *J. Appl. Phys.*, vol. 103, no. 7, p. 07C502, 2008.

[42] B. Hu, N. Amos, Y. Tian, J. Butler, D. Litvinov, and S. Khizroev, “Study of Co/Pd multilayers as a candidate material for next generation magnetic media,” *J. Appl. Phys.*, vol. 109, no. 3, p. 034314, Feb. 2011.

[43] P. S. Peercy, “The drive to miniaturization,” *Nature*, vol. 406, pp. 1023–6, Aug. 2000.

[44] J. Gregg, *Ones and Zeros: Understanding Boolean Algebra, Digital Circuits, and the Logic of Sets*. Hoboken, NJ: Wiley-IEEE Press, 1998.

[45] “Vacuum Tube Has Rival,” *Sci. News-Letter*, vol. 54, no. 2, p. 19, 1948.

[46] V. L. Safonov, “Logic Operations on a Hard Disk Drive,” Us 7,835,100 B2, 2010.

[47] J. Bardeen, “Research Leading to Point-Contact Transistor,” *Sci. (New York, N.Y.)1*, vol. 126, no. 3264, pp. 105–112, 1957.

[48] W. H. Brattain, “Surface Properties of Semiconductors,” *Science*, vol. 126, no. 3265, pp. 151–153, 1957.

[49] W. Shockley, “Transistor Physics,” *Am. Sci.*, vol. 42, no. 1, pp. 41–72, 1954.

[50] I. Grout, *Digital Systems Design with FPGAs and CPLDs*. Burlington, MA: Newnes, 2008.

[51] M. M. Mana, M. D. Ciletti, and M. M. Mano, *Digital Design*, 4th ed. Upper Saddle River, NJ: Prentice Hall, 2007.

[52] U. F. Gianola, “Possibilities of All-Magnetic Logic,” *J. Appl. Phys.*, vol. 32, no. 3, p. S27, 1961.

[53] D. R. Bennion, H. D. Crane, and D. Nitzan, *Digital Magnetic Logic*. New York, New York, USA: McGraw-Hill, 1969.

[54] R. J. Spain, “Controlled Domain Tip Propagation, Part I,” *J. Appl. Phys.*, vol. 37, no. 7, p. 2572, 1966.

[55] R. J. Spain, “Controlled Domain Tip Propagation, Part II,” *J. Appl. Phys.*, vol. 37, no. 7, p. 2584, 1966.

[56] R. J. Spain, H. I. Jauvtis, and F. T. Duben, “DOT memory systems,” in *AFIPS ’74 Proceedings of the May 6-10, 1974, national computer conference and exposition*, 1974, p. 841.

[57] S. Joo, T. Kim, S. H. Shin, J. Y. Lim, J. Hong, J. D. Song, J. Chang, H.-W. Lee, K. Rhie, S. H. Han, K.-H. Shin, and M. Johnson, “Magnetic-field-controlled reconfigurable semiconductor logic.,” *Nature*, vol. 494, no. 7435, pp. 72–6, Feb. 2013.

[58] A. Imre, G. Csaba, L. Ji, A. Orlov, G. H. Bernstein, and W. Porod, “Majority Logic Gate for Magnetic Quantum-Dot Cellular Automata,” *Science*, vol. 311, no. 5758, pp. 205–8, Jan. 2006.

[59] M. T. Niemier, X. S. Hu, M. Alam, G. Bernstein, W. Porod, M. Putney, and J. DeAngelis, “Clocking structures and power analysis for nanomagnet-based logic devices,” in *Low Power Electronics and Design (ISLPED), 2007 ACM/IEEE International Symposium on*, 2007, pp. 26–31.

[60] T. Windbacher, O. Triebl, D. Osintsev, A. Makarov, V. Sverdlov, and S. Selberherr, “Simulation study of an electrically read- and writable magnetic logic gate,” *Microelectron. Eng.*, vol. 112, pp. 188–192, Dec. 2013.

[61] I. Eichwald and J. Kiermaier, “Towards a signal crossing in double-layer nanomagnetic logic,” *IEEE Trans. Magn.*, vol. 49, no. 7, pp. 4468–4471, 2013.

[62] S. Breitkreutz, J. Kiermaier, I. Eichwald, C. Hildbrand, G. Csaba, D. Schmitt-Landsiedel, and M. Becherer, “Experimental Demonstration of a 1-Bit Full Adder in Perpendicular Nanomagnetic Logic,” *IEEE Trans. Magn.*, vol. 49, no. 7, pp. 4464–4467, Jul. 2013.

[63] R. Lavrijsen, J.-H. Lee, A. Fernández-Pacheco, D. C. M. C. Petit, R. Mansell, and R. P. Cowburn, “Magnetic ratchet for three-dimensional spintronic memory and logic.,” *Nature*, vol. 493, no. 7434, pp. 647–50, Jan. 2013.

[64] B. Lee, J. Hong, N. Amos, I. Dumer, D. Litvinov, and S. Khizroev, “Sub-10-nm-resolution electron-beam lithography toward very-high-density multilevel 3D nano-magnetic information devices,” *J. Nanoparticle Res.*, vol. 15, no. 6, p. 1665, May 2013.

[65] R. P. Cowburn, “Where Have All the Transistors Gone?,” *Science*, vol. 311, no. 5758, pp. 183–4, Jan. 2006.

[66] C. D. Mee and E. D. Daniel, *Magnetic Recording Technology*, 2nd ed. New York, New York, USA: McGraw-Hill Professional, 1996.

[67] D. A. Allwood, G. Xiong, M. D. Cooke, C. C. Faulkner, D. Atkinson, N. Vernier, and R. P. Cowburn, “Submicrometer ferromagnetic NOT gate and shift register.,” *Science*, vol. 296, no. 5575, pp. 2003–6, Jun. 2002.

[68] J. C. Slonczewski, “Current-driven excitation of magnetic multilayers,” *J. Magn. Magn. Mater.*, vol. 159, no. 1–2, pp. L1–L7, Jun. 1996.

[69] M. N. Baibich, J. M. Broto, A. Fert, F. N. Van Dau, F. Petroff, P. Etienne, G. Creuzel, A. Friederich, and J. Chazelas, “Giant Magnetoresistance of (001)Fe/(001)Cr Magnetic Superlattices,” *Phys. Rev. Lett.*, vol. 61, no. 21, pp. 2472–2475, Nov. 1988.

[70] C. E, J. Rantschler, S. Khizroev, and D. Litvinov, “Micromagnetics of signal propagation in magnetic cellular logic data channels,” *J. Appl. Phys.*, vol. 104, no. 5, p. 054311, 2008.

[71] A. Orlov, A. Imre, G. Csaba, L. Ji, W. Porod, and G. H. Bernstein, “Magnetic Quantum-Dot Cellular Automata: Recent Developments and Prospects,” *J. Nanoelectron. Optoelectron.*, vol. 3, no. 1, pp. 55–68, Mar. 2008.

[72] D. C. Ralph and M. D. Stiles, "Spin transfer torques," *J. Magn. Magn. Mater.*, vol. 320, no. 7, pp. 1190–1216, Apr. 2008.

[73] S. Liu, X. S. Hu, M. T. Niemier, J. J. Nahas, G. Csaba, G. H. Bernstein, and W. Porod, "Exploring the Design of the Magnetic―Electrical Interface for Nanomagnet Logic," *IEEE Trans. Nanotechnol.*, vol. 12, no. 2, pp. 203–214, 2013.

[74] H. Mahmoudi, T. Windbacher, V. Sverdlov, and S. Selberherr, "Reliability Analysis and Comparison of Implication and Reprogrammable Logic Gates in Magnetic Tunnel Junction Logic Circuits," *IEEE Trans. Magn.*, vol. 49, no. 12, pp. 5620–5628, Dec. 2013.

[75] J. Z. Sun and D. C. Ralph, "Magnetoresistance and spin-transfer torque in magnetic tunnel junctions," *J. Magn. Magn. Mater.*, vol. 320, no. 7, pp. 1227–1237, Apr. 2008.

[76] T. Tanaka, Y. Otsuka, Y. Furomoto, K. Matsuyama, and Y. Nozaki, "Selective magnetization switching with microwave assistance for three-dimensional magnetic recording," *J. Appl. Phys.*, vol. 113, no. 14, p. 143908, 2013.

[77] N. Amos, J. Butler, B. Lee, M. H. Shachar, B. Hu, Y. Tian, J. Hong, D. Garcia, R. M. Ikkawi, R. C. Haddon, D. Litvinov, and S. Khizroev, "Multilevel-3D Bit Patterned Magnetic Media with 8 Signal Levels Per Nanocolumn," *PLoS One*, vol. 7, no. 7, p. e40134, Jan. 2012.

[78] D. Litvinov, V. Parekh, E. Chunsheng, D. Smith, J. Rantschler, P. Ruchhoeft, D. Weller, S. Khizroev, and C. E, "Nanoscale Bit-Patterned Media for Next Generation Data Storage Systems," *J. Nanoelectron. Optoelectron.*, vol. 3, no. 2, pp. 93–112, Jul. 2008.

[79] "OOMMF." [Online]. Available: http://math.nist.gov/oommf/.

[80] S. Iwasaki and Y. Nakamura, "An analysis for the magnetization mode for high density magnetic recording," *IEEE Trans. Magn.*, vol. 13, no. 5, pp. 1272–1277, 1977.

[81] M. C. B. Parish and M. Forshaw, "Physical constraints on magnetic quantum cellular automata," *Appl. Phys. Lett.*, vol. 83, no. 10, p. 2046, 2003.

[82] E. B. Svedberg, R. J. M. van de Veerdonk, K. J. Howard, and L. D. Madsen, "Quantifiable combinatorial materials science approach applied to perpendicular magnetic recording media," *J. Appl. Phys.*, vol. 93, no. 9, p. 5519, 2003.